COMMUNICATIONS IN COMPUTATIONAL PHYSICS
Vol. **2**, No. 6, pp. 1139-1173

Commun. Comput. Phys.
December 2007

High Performance Algorithms Based on a New Wavelet Expansion for Time Dependent Acoustic Obstacle Scattering

Lorella Fatone[1], Giuseppe Rao[2], Maria Cristina Recchioni[3] and Francesco Zirilli[4,*]

[1] *Dipartimento di Matematica Pura e Applicata, Università di Modena e Reggio Emilia, Via Campi 213/b, 41100 Modena, Italy.*
[2] *Dipartimento di Matematica e Applicazioni, Università di Palermo, Via Archirafi 34, 90123 Palermo, Italy.*
[3] *Dipartimento di Scienze Sociali "D. Serrani", Università Politecnica delle Marche, Piazza Martelli 8, 60121 Ancona, Italy.*
[4] *Dipartimento di Matematica "G. Castelnuovo", Università di Roma "La Sapienza", Piazzale Aldo Moro 2, 00185 Roma, Italy.*

Received 15 December 2006; Accepted (in revised version) 20 March 2007

Communicated by Gang Bao

Available online 15 June 2007

Abstract. This paper presents a highly parallelizable numerical method to solve time dependent acoustic obstacle scattering problems. The method proposed is a generalization of the "operator expansion method" developed by Recchioni and Zirilli [SIAM J. Sci. Comput., 25 (2003), 1158-1186]. The numerical method proposed reduces, via a perturbative approach, the solution of the scattering problem to the solution of a sequence of systems of first kind integral equations. The numerical solution of these systems of integral equations is challenging when scattering problems involving realistic obstacles and small wavelengths are solved. A computational method has been developed to solve these challenging problems with affordable computing resources. To this aim a new way of using the wavelet transform and new bases of wavelets are introduced, and a version of the operator expansion method is developed that constructs directly element by element in a fully parallelizable way. Several numerical experiments involving realistic obstacles and "small" wavelengths are proposed and high dimensional vector spaces are used in the numerical experiments. To evaluate the performance of the proposed algorithm on parallel computing facilities, appropriate speed up factors are introduced and evaluated.

AMS subject classifications: 34L25, 01-08

Key words: Time dependent acoustic scattering, Helmholtz equation, integral equation methods, wavelet bases, sparse linear systems.

*Corresponding author. *Email address:* f.zirilli@caspur.it (F. Zirilli)

1 Introduction

In this paper, we present a new version of the operator expansion method that improves the method developed in [1]. Roughly speaking, the operator expansion method is used to solve an exterior boundary value problem for the Helmholtz equation by reducing it to a sequence of systems of first kind integral equations defined on a suitable reference surface. Three innovations are introduced:

1) the use of the wavelet transform in a way different from that suggested in [1] that allows us to compute the coefficient matrices of the systems of linear equations mentioned above element by element in a fully parallelizable way;
2) new bases of wavelets with an (arbitrary) assigned number of vanishing moments that generalize the Haar's basis;
3) the representation on these wavelet bases of the integral operators, the unknowns and the data of the systems of integral equations obtained with the operator expansion method in order to approximate the integral equations with sparse systems of linear equations.

These innovations make the development of a highly parallelizable numerical method possible to deal with scattering problems involving obstacles having complex shapes and wavelengths small when compared to the characteristic dimensions of the obstacles. That is, problems that require the use of a large number of unknowns and equations can be discretized satisfactorily. In fact, thank to the representation of the integral operators on the wavelet bases and to a simple truncation procedure, matrices that approximate the integral operators with a very high sparsity factor are obtained. Consequently, high dimensional problems in the discretized variables can be solved at an affordable computational cost.

Let us begin by introducing some notation. Let $\mathbb{R}$ be the set of real numbers, $\mathbb{R}^h$ be the h-dimensional real Euclidean space, and $\underline{x}=(x_1,x_2,\cdots,x_h)^T\in\mathbb{R}^h$ a generic vector. Let $(\cdot,\cdot)$ and $\|\cdot\|$ denote the Euclidean scalar product and the corresponding Euclidean vector norm respectively.

Let $\mathbf{C}$ be the complex numbers. For $z\in\mathbf{C}$ we denote with $Re(z)$ and $Im(z)$ the real and imaginary parts of z respectively. We denote with $\mathbf{C}^h$ the h dimensional complex Euclidean space.

Let $\Omega\subset\mathbb{R}^3$ be a bounded simply connected open set with locally Lipschitz boundary $\partial\Omega$ and let $\overline{\Omega}$ be its closure. Furthermore we denote with $\underline{n}(\underline{x})=(n_1(\underline{x}),n_2(\underline{x}),n_3(\underline{x}))^T\in\mathbb{R}^3$ the outward unit normal vector to $\partial\Omega$ in $\underline{x}\in\partial\Omega$. We note that when $\partial\Omega$ is a locally Lipschitz surface the unit normal vector $\underline{n}(\underline{x})$ exists almost everywhere in $\underline{x}$ when $\underline{x}\in\partial\Omega$ (see [2, Theorem 1.8 p. 17 and p. 52]).

We assume that $\partial\Omega$ can be decomposed as follows: $\partial\Omega=\partial\Omega_1\cup\partial\Omega_2$, where $\partial\Omega_1$, $\partial\Omega_2$ are two locally Lipschitz surfaces such that $\partial\Omega_1\cap\partial\Omega_2=\emptyset$. Finally we assume that $\partial\Omega_1$ is characterized by a boundary acoustic impedance given by a bounded continuous non-negative real function $\chi=\chi(\underline{x})$, $\underline{x}\in\partial\Omega_1$, and that $\partial\Omega_2$ is characterized by an infinite

boundary acoustic impedance, that is, $\chi=\chi(\underline{x})=+\infty$, $\underline{x}\in\partial\Omega_2$, that is, $\partial\Omega_2$ is an acoustically hard boundary. Moreover, for later convenience, we assume that Ω contains the origin of the coordinate system.

We are interested in the solution of the following boundary value problem for the Helmholtz equation:

$$\Delta u_k^s(\underline{x})+k^2u_k^s(\underline{x})=0,\quad \underline{x}\in\mathbb{R}^3\setminus\overline{\Omega}, \tag{1.1}$$

with the boundary conditions:

$$u_k^s(\underline{x})+\frac{\chi(\underline{x})}{\imath k}\frac{\partial u_k^s}{\partial\underline{n}}(\underline{x})=g_{1,k}(\underline{x}),\quad \underline{x}\in\partial\Omega_1, \tag{1.2}$$

$$\frac{\partial u_k^s}{\partial\underline{n}}(\underline{x})=g_{2,k}(\underline{x}),\quad \underline{x}\in\partial\Omega_2, \tag{1.3}$$

and the Sommerfeld radiation condition:

$$\frac{\partial u_k^s}{\partial r}(\underline{x})-\imath ku_k^s(\underline{x})=o(r^{-1}),\quad r\to+\infty, \tag{1.4}$$

where $k\in\mathbb{R}$ is the wave number, $k\neq0$, $\imath$ is the imaginary unit, $g_{1,k}(\underline{x})$, $\underline{x}\in\partial\Omega_1$, $g_{2,k}(\underline{x})$, $\underline{x}\in\partial\Omega_2$ are given functions, $r=\|\underline{x}\|$, $\underline{x}\in\mathbb{R}^3$. Moreover, we denote with $o(\cdot)$ and later on with $\mathcal{O}(\cdot)$ the Landau symbols. When $k=0$, problem (1.1)-(1.4), after being rewritten, can be approached with a simple adaptation of the method presented in this paper. The development of a highly performing solver for problem (1.1)-(1.4) is a relevant task in many applications and has been considered by several authors (see, e.g., [3–5]). The fast multipole algorithms [3–5] are very successful methods for problem (1.1)-(1.4). In Section 3, we make a comparison between the algorithm proposed in this paper and the fast multipole algorithms in terms of computational cost.

The first step in the development of the solver of (1.1)-(1.4) proposed here is the reduction of the boundary value problem (1.1)-(1.4) to a system of integral equations. This step, when $\partial\Omega$ is a sufficiently regular surface, is usually done by introducing a boundary integral method. For reasons explained in [1, 6] we prefer not to use boundary integral methods and instead we develop an operator expansion method for problem (1.1)-(1.4). In this way problem (1.1)-(1.4) is transformed to a sequence of systems of integral equations under the following assumptions (see [1]):

(a) there exists a bounded simply connected open set Ω_c such that $\partial\Omega_c$ is a sufficiently regular surface, $\overline{\Omega}_c\subset\Omega$ and such that the solution $u_k^s(\underline{x})$ of (1.1)-(1.4) defined for $\underline{x}\in\mathbb{R}^3\setminus\overline{\Omega}$ can be extended to $\underline{x}\in\mathbb{R}^3\setminus\overline{\Omega}_c$ remaining a solution of the Helmholtz equation in $\mathbb{R}^3\setminus\overline{\Omega}_c$. We assume that the origin belongs to Ω_c. To keep the notation simple we omit the (possible) dependence on k of Ω_c when $k\in\mathbb{R}$, $k\neq0$;

(b) for $k\in\mathbb{R}$, $k\neq0$, $F_k(\underline{x})$, the extension of $u_k^s(\underline{x})$ whose existence is assumed in (a), can be represented as a single layer potential with density supported on $\partial\Omega_c$, that is:

$$F_k(\underline{x})=\int_{\partial\Omega_c}\Phi_k(\underline{x},\underline{y})v_k(\underline{y})ds(\underline{y}),\quad \underline{x}\in\mathbb{R}^3\setminus\overline{\Omega}_c, \tag{1.5}$$

where ds is the surface measure on $\partial\Omega_c$ (see [2, Theorem 1.2 p.15]), $v_k(\underline{y})$, $\underline{y}\in\partial\Omega_c$, is a density function to be determined, and Φ_k is the fundamental solution of the Helmholtz equation in $\mathbb{R}^3$ with the Sommerfeld radiation condition at infinity:

$$\Phi_k(\underline{x},\underline{y})=\frac{e^{\imath k\|\underline{x}-\underline{y}\|}}{4\pi\|\underline{x}-\underline{y}\|},\quad \underline{x}\neq\underline{y},\quad \underline{x},\underline{y}\in\mathbb{R}^3. \tag{1.6}$$

The single layer potential (1.5) satisfies equations (1.1), (1.4) for every choice of v_k that makes possible the differentiation of (1.5) under the integral sign. So that, we can reformulate problem (1.1)-(1.4) as a system of integral equations in the unknown v_k imposing that F_k satisfies the boundary conditions (1.2) and (1.3):

$$\int_{\partial\Omega_c}\Phi_k(\underline{x},\underline{y})v_k(\underline{y})ds(\underline{y})+\frac{\chi(\underline{x})}{\imath k}\frac{\partial}{\partial\underline{n}(\underline{x})}\int_{\partial\Omega_c}\Phi_k(\underline{x},\underline{y})v_k(\underline{y})ds(\underline{y})=g_{1,k}(\underline{x}),\quad \underline{x}\in\partial\Omega_1, \tag{1.7}$$

$$\frac{\partial}{\partial\underline{n}(\underline{x})}\int_{\partial\Omega_c}\Phi_k(\underline{x},\underline{y})v_k(\underline{y})ds(\underline{y})=g_{2,k}(\underline{x}),\quad \underline{x}\in\partial\Omega_2. \tag{1.8}$$

In this way, we have reformulated the boundary value problem (1.1)-(1.4) in the unknown u_k^s as a system of integral equations in the unknown v_k. Since we have chosen $\overline{\Omega}_c\subset\Omega$ the distance between $\partial\Omega_c$ and $\partial\Omega$ is greater than zero so that the integral equations (1.7)-(1.8) have continuous kernels defining compact operators even when $\partial\Omega$ and $\partial\Omega_c$ are only Lipschitz continuous surfaces. That is, they are Fredholm integral equations of the first kind which are known to be ill posed.

The "operator expansion method" tries to take care of the ill-posedness of the integral equations (1.7)-(1.8) via a perturbative approach. That is, the unknown v_k and the kernels of (1.7)-(1.8) are represented through a perturbative expansion having as base point a sufficiently regular surface $\partial\Omega_r$, boundary of a bounded simply connected open set Ω_r. The set Ω_r is chosen such that: i) $\overline{\Omega}_c\subset\Omega_r$, ii) the "distances" between $\partial\Omega$ and $\partial\Omega_r$ and between $\partial\Omega_r$ and $\partial\Omega_c$ are small. Note that the natural unit to measure these distances is the wavelength $\lambda=2\pi/k$. We assume that $\partial\Omega$, $\partial\Omega_c$, $\partial\Omega_r$ can be represented by using single valued functions in a given (curvilinear) coordinate system. By requiring that (1.7)-(1.8) are satisfied order by order in the perturbation expansion when $\partial\Omega$ "goes to" $\partial\Omega_r$, the solution of (1.7)-(1.8) is reduced to the solution of a sequence of systems of integral equations. Finally representing the integral operators, the unknowns and the data of the resulting sequence of systems of integral equations on a wavelet basis and using a simple truncation procedure, the problem of solving the systems of integral equations obtained by expanding (1.7)-(1.8) is approximated with the problem of solving sparse systems of linear equations. The choice of the surfaces $\partial\Omega_r$ and $\partial\Omega_c$ plays an important role, that will be discussed in Section 4, in the treatment of the ill-conditioning of (1.7)-(1.8) and in making sparse the coefficient matrices of the linear systems that approximate the integral equations.

Note that the assumptions made above, to develop the operator expansion, are made for convenience in order to keep the exposition simple. The assumptions (a), (b), $i)$ and

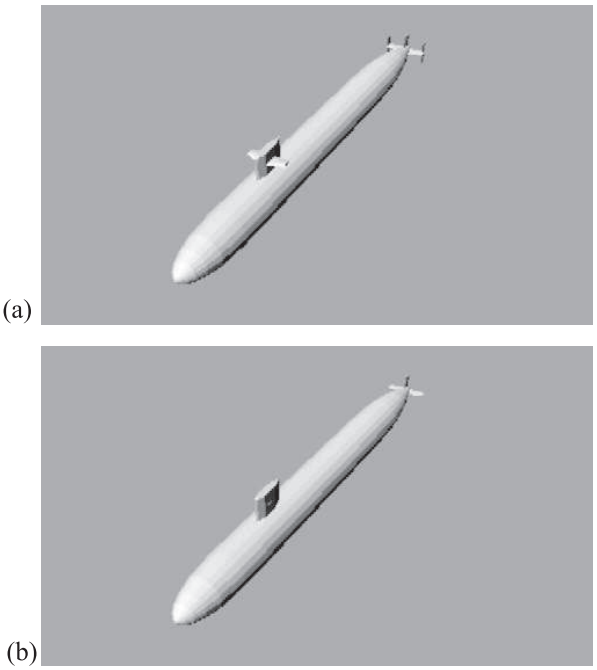

Figure 1: Submarine (a) and its simplified version (b).

ii) in practice are not really restrictive. In fact our purpose is to approximate the solution u_k^s of problem (1.1)-(1.4) and it is possible to show (see [7, Theorem 2.1 p. 588] for the case $\partial\Omega_1=\partial\Omega$, $\chi(\underline{x})=0$, $\underline{x}\in\partial\Omega$, $\partial\Omega_2=\emptyset$) that under some hypotheses on the surface $\partial\Omega_c$ the set of the data generated by the single layer potentials F_k when the density v_k is a square integrable function over $\partial\Omega_c$ is a dense subset of the square integrable functions over $\partial\Omega$.

On the contrary, the assumption that $\partial\Omega$, $\partial\Omega_c$ and $\partial\Omega_r$ can be represented with single valued functions in an (unique) "easy to use" curvilinear coordinate system is restrictive. In fact, for example, this last assumption forces us to "simplify" some of the obstacles considered in the numerical experiments shown in Section 4 (see Figs. 1 and 2). Indeed we can avoid this assumption and the consequent "simplifications" using an operator expansion method that uses more than one curvilinear coordinate system to represent the relevant boundaries (see [8]). In this paper, in order to keep the exposition and the computer programs used simple, we restrict our attention on the scattering problems involving the simplified versions of the realistic obstacles proposed in Fig. 1(a) and Fig. 2(a) that can be solved using only one curvilinear coordinate system.

Moreover, we use the solver of the exterior boundary value problem for the Helmholtz equation (1.1)-(1.4) developed here as a computational tool in the solution of the following time dependent scattering problem. Let t be the time variable and $u^i(\underline{x},t)$, $(\underline{x},t)\in\mathbb{R}^3\times\mathbb{R}$, be an incoming acoustic field propagating with velocity $c>0$ in a homogeneous isotropic medium filling $\mathbb{R}^3$, solution of the wave equation (1.9) in $\mathbb{R}^3\times\mathbb{R}$. When u^i hits the obstacle Ω, a scattered wave $u^s(\underline{x},t)$, $(\underline{x},t)\in(\mathbb{R}^3\setminus\overline{\Omega})\times\mathbb{R}$, is generated and u^s is the

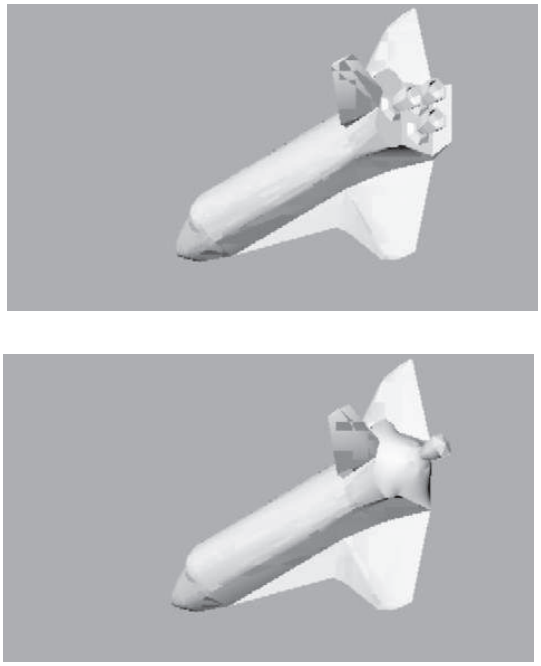

Figure 2: NASA space shuttle (a) and its simplified version (b).

solution of the following problem (see [6]):

$$\Delta u^s(\underline{x},t)-\frac{1}{c^2}\frac{\partial^2 u^s}{\partial t^2}(\underline{x},t)=0,\quad (\underline{x},t)\in(\mathbb{R}^3\setminus\overline{\Omega})\times\mathbb{R}, \tag{1.9}$$

with the boundary conditions (see [10, p. 66]):

$$-\frac{\partial u^s}{\partial t}(\underline{x},t)+c\chi(\underline{x})\frac{\partial u^s}{\partial \underline{n}(\underline{x})}(\underline{x},t)=g_1(\underline{x},t),\quad (\underline{x},t)\in\partial\Omega_1\times\mathbb{R}, \tag{1.10}$$

$$\frac{\partial u^s}{\partial \underline{n}(\underline{x})}(\underline{x},t)=g_2(\underline{x},t),\quad (\underline{x},t)\in\partial\Omega_2\times\mathbb{R}, \tag{1.11}$$

where g_1, g_2 are given by:

$$g_1(\underline{x},t)=\frac{\partial u^i}{\partial t}(\underline{x},t)-c\chi(\underline{x})\frac{\partial u^i}{\partial \underline{n}(\underline{x})}(\underline{x},t),\quad (\underline{x},t)\in\partial\Omega_1\times\mathbb{R}, \tag{1.12}$$

$$g_2(\underline{x},t)=-\frac{\partial u^i}{\partial \underline{n}(\underline{x})}(\underline{x},t),\quad (\underline{x},t)\in\partial\Omega_2\times\mathbb{R}, \tag{1.13}$$

with the boundary condition at infinity:

$$u^s(\underline{x},t)=\mathcal{O}(r^{-1}),\quad r\to\infty,\quad t\in\mathbb{R}, \tag{1.14}$$

and the radiation condition:

$$\frac{\partial u^s}{\partial r}(\underline{x},t)+\frac{1}{c}\frac{\partial u^s}{\partial t}(\underline{x},t)=\mathcal{O}(r^{-1}),\quad r\to\infty,\quad t\in\mathbb{R}. \tag{1.15}$$

Note that conditions (1.10)-(1.11) and similar conditions (1.2)-(1.3) contain the limit cases of the acoustically hard obstacle and of the acoustically soft obstacle. The boundary condition at infinity (1.14) and the radiation condition (1.15) imply respectively that $u^s(\underline{x},t)$ goes to zero as $r\to+\infty$ and that $u^s(\underline{x},t)$ is made to leading order of outgoing waves. In fact we can think the scattered field $u^s(\underline{x},t)$ as a superposition of outgoing waves having their sources on $\partial\Omega$. Let $B=\{\underline{x}\in\mathbb{R}^3\,|\,\|\underline{x}\|<1\}$, and ∂B be the boundary of B. Since $u^i(\underline{x},t)$ satisfies the wave equation in $\mathbb{R}^3\times\mathbb{R}$, it can be represented as a linear superposition of time harmonic waves of the form $e^{-\imath\omega t}u^i_{\frac{\omega}{c},\underline{\alpha}}(\underline{x})$ where $u^i_{\frac{\omega}{c},\underline{\alpha}}(\underline{x})=e^{\imath\frac{\omega}{c}(\underline{x},\underline{\alpha})}$, $\omega\in\mathbb{R}$, $\underline{\alpha}\in\partial B$, so that we can assume that $u^s(\underline{x},t)$ has a similar form, that is, $u^s(\underline{x},t)$ is a linear superposition of time harmonic waves (see Section 3 and [6] for further details), which can be approximated as follows:

$$u^s(\underline{x},t)\approx\sum_{i=1}^{N_1}\sum_{j=1}^{N_2}a_{i,j}e^{-\imath\omega_i t}u^s_{\frac{\omega_i}{c},\underline{\alpha}_j}(\underline{x}),\quad(\underline{x},t)\in(\mathbb{R}^3\setminus\overline{\Omega})\times\mathbb{R}, \tag{1.16}$$

where N_1, N_2 are two positive integers, $\omega_i\in\mathbb{R}$, $a_{i,j}\in\mathbb{R}$, $\underline{\alpha}_j\in\partial B$, and $u^s_{\frac{\omega_i}{c},\underline{\alpha}_j}(\underline{x})$ are functions to be determined. Thank to formula (1.16), we can approximate the solution of problem (1.9)-(1.15) with the solution of $N_1\cdot N_2$ problems of type (1.1)-(1.4). That is, in order to obtain an approximation of the solution of problem (1.9)-(1.15), we must solve $N_1\cdot N_2$ boundary value problems for the Helmholtz equation (1.1)-(1.4). These last problems can be approached with the operator expansion method introduced in this paper.

Note that, when realistic obstacles Ω and wavelengths small compared to the characteristic dimensions of the obstacles are considered, in order to have a satisfactory accuracy in the solution, the integral equations resulting from the operator expansion must be discretized using finite dimensional vector spaces of high dimension. The operator expansion method developed here can handle this situation by improving the operator expansion method proposed in [1] in several respects. Moreover the operator expansion method proposed here is highly parallelizable so that the computation of the entries of the matrices that represent the integral operators in the wavelet basis can be done element by element with independent computations. In the operator expansion method proposed in [1] this was not the case due to the way in which the wavelet transform was used. The way of using the wavelet transform was also responsible for the severe memory requirements of the method proposed in [1] when high dimensional discretized problems were considered.

The operator expansion method has been widely used to solve problems in acoustic and electromagnetic scattering, see, e.g., [6,11–17]. It was originally introduced by Milder to solve acoustic and electromagnetic scattering problems from open surfaces [11, 12] and later has been adapted to solve acoustic and electromagnetic scattering problems

from bounded obstacles [13–17]. Recently it has been used in the solution of control problems for partial differential equations in acoustics and electromagnetics motivated by the attempt of finding active strategies to avoid the recognition of an obstacle from the observation of its scattered field [18–22]. The operator expansion method developed in this paper makes possible to solve control problems involving "realistic" obstacles and "small" wavelengths.

In Section 2, we construct the generalized Haar's wavelets, and in Section 3, we present the new version of the operator expansion method to solve (1.1)-(1.4) that uses the wavelet bases introduced in Section 2 and the corresponding computational method. For simplicity, in Sections 2 and 3, we restrict our exposition to the case of obstacles with a bounded boundary acoustic impedance, that is $\partial\Omega_1=\partial\Omega$, $\partial\Omega_2=\emptyset$, when $k\neq 0$ but the general case can be treated analogously. Furthermore in Section 3, we show how the new version of the operator expansion method can be used to compute the solution of the time dependent acoustic obstacle scattering problem (1.9)-(1.15). In Section 4, we present some numerical results obtained with the method presented in Section 3. In particular we solve time dependent acoustic scattering problems involving realistic objects including a simplified version of a submarine (see Fig. 1(b)) and a simplified version of the NASA space shuttle (see Fig. 2(b)). The parallel performance of the numerical algorithm used is studied.

2 The wavelet bases

Let $L^2((0,1))$ be the space of the square integrable real functions defined on the interval $(0,1)$. The wavelet bases we propose are bases of $L^2((0,1))$ that generalize the Haar's basis ([9] p. 10) that, to our knowledge, have not been used before. These wavelet bases are made of piecewise polynomial functions. The polynomials used in the numerical experience shown in Section 4 are of low degree making the computation particularly efficient.

The procedure that constructs these bases is implementable using a symbolic programming language such as Mathematica or Symbolic Matlab and takes as input parameters the number M of vanishing moments of the wavelet basis considered, the number N of subintervals of the interval $(0,1)$ employed and the points $\eta_i\in(0,1)$, $i=1,2,\cdots,N-1$, where the subdivision of $(0,1)$ in subintervals takes place, we assume that $\eta_i<\eta_{i+1}$, $i=1,2,\cdots,N-2$. That is we assume M and N to be two integers such that $M\geq 1$ and $N\geq 2$ and we denote with $P^M((0,1))$ the space of the polynomials of degree less than M defined on $(0,1)$. We consider the following decomposition of $L^2((0,1))$:

$$L^2((0,1))=P^M((0,1))\oplus V^M((0,1)), \tag{2.1}$$

where $\oplus$ denotes the direct sum of subspaces. In other words, $V^M((0,1))$ and $P^M((0,1))$

are orthogonal closed subspaces of $L^2((0,1))$, such that:

$$\begin{aligned}&\text{the vector space generated by the union of}\\&P^M((0,1)) \text{ and } V^M((0,1)) \text{ is } L^2((0,1)),\end{aligned} \tag{2.2}$$

so that we have:

$$\int_0^1 dx\, f(x)g(x)=0, \quad \forall f\in P^M((0,1)), \quad g\in V^M((0,1)), \tag{2.3}$$

and

$$P^M((0,1))\cap V^M((0,1))=\{0\}. \tag{2.4}$$

We choose as basis of $P^M((0,1))$ the first M Legendre orthonormal polynomials defined on $(0,1)$ and we refer to them as $L_j(x)$, $x\in(0,1)$, $j=0,1,\cdots,M-1$.

We construct a basis of $V^M((0,1))$ using the multiresolution analysis introduced by Mallat [23] and Meyer [24]. Let $N\geq 2$ be an integer and $\underline{\eta}^N=(\eta_1,\eta_2,\cdots,\eta_{N-1})^T\in\mathbb{R}^{N-1}$.

For M, N positive integers such that $M\geq 1$, $N\geq 2$ we define the following piecewise polynomial functions on $(0,1)$: for $1\leq i\leq N-2$ and $0\leq j\leq (N-1)M-1$,

$$\Psi^M_{j,N,\underline{\eta}^N}(x)=\begin{cases} p^M_{1,j,N,\underline{\eta}^N}(x), & x\in(0,\eta_1),\\ p^M_{i+1,j,N,\underline{\eta}^N}(x), & x\in[\eta_i,\eta_{i+1}),\\ p^M_{N,j,N,\underline{\eta}^N}(x), & x\in[\eta_{N-1},1),\end{cases} \tag{2.5}$$

where

$$p^M_{i,j,N,\underline{\eta}^N}(x)=\sum_{l=0}^{M-1} q_{l,i,j,M,N,\underline{\eta}^N}x^l\in P^M((0,1))$$

are polynomials of degree less than M.

We determine the coefficients $q_{l,i,j,M,N,\underline{\eta}^N}$ of $p^M_{i,j,N,\underline{\eta}^N}$ by imposing the following conditions:

$$\int_0^1 dx\,\Psi^M_{j,N,\underline{\eta}^N}(x)x^l=0, \quad l=0,1,\cdots,M-1, \quad j=0,1,\cdots,(N-1)M-1, \tag{2.6}$$

$$\int_0^1 dx\,\Psi^M_{j,N,\underline{\eta}^N}(x)\Psi^M_{j',N,\underline{\eta}^N}(x)=\begin{cases}0, & j\neq j',\\ 1, & j=j',\end{cases} \quad j,j'=0,1,\cdots,(N-1)M-1. \tag{2.7}$$

We note that in general conditions (2.6) and (2.7) define $(N-1)(M^2+((N-1)M^2+M)/2$ distinct equations in the $N(N-1)M^2$ unknowns $q_{l,i,j,M,N,\underline{\eta}^N}$. Note that when $M=1$ and $N=2$ the number of equations is equal to the number of unknowns and the unknown coefficients are uniquely determined up to a sign permutation. However, when $M>1$ (and $N\geq 2$) the number of equations is smaller than the number of unknowns. In this case, we must choose the undetermined unknowns according to some criterion. For example a

possible criterion consists in imposing some regularity to the piecewise polynomial functions $\Psi^M_{j,N,\underline{\eta}^N}$. The functions $\Psi^M_{j,N,\underline{\eta}^N}$ can be interpreted as "wavelet mother functions" and we generate the elements of the wavelet basis associated to them via the multiresolution approach (see [23,24]).

To keep the exposition simple, from now on we choose $N=2$, $\eta_i=i/N$, $i=1,\cdots,N-1$. Results analogous to the ones obtained here can be derived for the general choice of η_i.

Let us define the functions:

$$\psi^M_{j,m,\nu,N,\underline{\eta}^N}(x)=\begin{cases} N^{\frac{m}{2}}\Psi^M_{j,N,\underline{\eta}^N}(N^m x-\nu), & x\in(\nu N^{-m},(\nu+1)N^{-m}),\\ 0, & x\in(0,1)\setminus(\nu N^{-m},(\nu+1)N^{-m}),\end{cases} \tag{2.8a}$$

$$(\nu,m,j)\in\Lambda:=\{\nu=0,1,\cdots,N^m-1,\ m=0,1,\cdots,\ j=0,1,\cdots,M-1\}, \tag{2.8b}$$

and the set of functions $W^M_{N,\underline{\eta}^N}((0,1))$:

$$W^M_{N,\underline{\eta}^N}((0,1))=\left\{L_j(x),\ \psi^M_{j,m,\nu,N,\underline{\eta}^N}(x),\ x\in(0,1),(\nu,m,j)\in\Lambda\right\}, \tag{2.9}$$

where $L_j(x)$ are the Legendre polynomials and $\Psi^M_{j,N,\underline{\eta}^N}(x)$ are defined by (2.5) when we choose $\underline{\eta}^N=(1/N,2/N,\cdots,(N-1)/N)^T$. Note that the function $\psi^M_{j,m,\nu,N,\underline{\eta}^N}(x)$ has support given by the interval $(\nu N^{-m},(\nu+1)N^{-m})\subset(0,1)$.

In the Appendix we show that the set $W^M_{N,\underline{\eta}^N}$ is an orthonormal basis of $L^2((0,1))$ and that some classes of integral kernels can be efficiently approximated using these bases.

We note that when $M=1$ and, as chosen previously, $N=2$ the set of functions defined in (2.9) is the well known Haar's basis (see [9] p. 10) and that when $M>1$, $N=2$ the set of functions defined in (2.9) is the generalization of the Haar's basis.

Furthermore it is easy to see that the functions $\Psi^M_{j,N,\underline{\eta}^N}$ are determined up to a sign permutation when we impose conditions (2.6)-(2.7) and use the fact that $\Psi^M_{j,N,\underline{\eta}^N}\in C^{j-1}((0,1))$. That is:

$$\frac{d^\nu}{dx^\nu}p^M_{i,j,N,\underline{\eta}^N}(\eta_i^-)=\frac{d^\nu}{dx^\nu}p^M_{i+1,j,N,\underline{\eta}^N}(\eta_i^+),\quad 1\le i\le N-1,\ 0\le\nu\le j-1,\ 1\le j\le M-1. \tag{2.10}$$

The conditions given in (2.10) are one possible choice of the criterion to determine the coefficients left undetermined by (2.6)-(2.7). We denote with $\widehat{\Psi}^M_{j,N,\underline{\eta}^N}$ a choice of the functions $\Psi^M_{j,N,\underline{\eta}^N}$ satisfying condition (2.10), with $\widehat{\psi}^M_{j,m,\nu,N,\underline{\eta}^N}$ the functions defined in (2.8) when we replace $\Psi^M_{j,N,\underline{\eta}^N}$ with $\widehat{\Psi}^M_{j,N,\underline{\eta}^N}$, and with $\widehat{W}^M_{N,\underline{\eta}^N}((0,1))$ the corresponding basis whose elements are L_j and $\widehat{\psi}^M_{j,m,\nu,N,\underline{\eta}^N}$.

Let us rename the functions belonging to the basis $W^M_{N,\underline{\eta}^N}((0,1))$ of $L^2((0,1))$ defined in (2.9) as follows:

$$\tilde{\psi}^M_{j,m,\nu,N,\underline{\eta}^N}(x)=\psi^M_{j,m,\nu,N,\underline{\eta}^N}(x),\ x\in(0,1),\ (\nu,m,j)\in\Lambda, \tag{2.11a}$$

$$\tilde{\psi}^M_{j,m,\nu,N,\underline{\eta}^N}(x)=L_{-j-1}(x),\ x\in(0,1),\ -M\le j\le-1,\ m=\nu=0. \tag{2.11b}$$

Using two copies of a basis of $L^2((0,1))$ chosen between those defined in (2.9), and taking the tensor product of the basis functions we can construct a wavelet basis of $L^2((0,1)\times(0,1))$, denoted with $W^M_{N,\underline{\eta}^N}((0,1)\times(0,1))$, that is:

$$\begin{aligned}
&W^M_{N,\underline{\eta}^N}((0,1)\times(0,1))\\
=&\Big\{\tilde{\Upsilon}^M_{j,m,\nu,j',m',\nu',N,\underline{\eta}^N}(x,y)=\tilde{\psi}^M_{j,m,\nu,N,\underline{\eta}^N}(x)\tilde{\psi}^M_{j',m',\nu',N,\underline{\eta}^N}(y),\\
&\quad (x,y)\in(0,1)\times(0,1),\quad -M\le j,j'\le M-1,\quad \text{and } m=0 \text{ when } j<0;\\
&\quad m=0,1,\cdots \text{ when } j\ge 0;\quad m'=0 \text{ when } j'<0;\quad m'=0,1,\cdots \text{ when } j'\ge 0;\\
&\quad \nu=0,1,\cdots(N^m-1)_+,\quad \nu'=0,1,\cdots,(N^{m'}-1)_+\Big\},
\end{aligned}\tag{2.12}$$

where $(*)_+$ denotes the maximum between 0 and $*$.

Let (a,b), $(a',b')\subset\mathbb{R}$ be two bounded intervals. We will describe the wavelet bases of $L^2((a,b)\times(a',b'))$ that will be used in the numerical experiments of Section 4.

We define the required wavelet bases of $L^2((a,b)\times(a',b'))$ as follows:

$$\begin{aligned}
&W^M_{N,\underline{\eta}^N}\big((a,b)\times(a',b')\big)\\
=&\Big\{\Upsilon^M_{j,m,\nu,j',m',\nu',N,\underline{\eta}^N}(x,y)=\frac{1}{\sqrt{b-a}}\tilde{\psi}^M_{j,m,\nu,N,\underline{\eta}^N}\left(\frac{x-a}{b-a}\right)\frac{1}{\sqrt{b'-a'}}\tilde{\psi}^M_{j',m',\nu',N,\underline{\eta}^N}\left(\frac{y-a'}{b'-a'}\right),\\
&\quad (x,y)\in(0,1)\times(0,1),\quad -M\le j,j'\le M-1,\quad \text{and } m=0 \text{ when } j<0;\\
&\quad m=0,1,\cdots \text{ when } j\ge 0;\quad m'=0 \text{ when } j'<0;\quad m'=0,1,\cdots \text{ when } j'\ge 0;\\
&\quad \nu=0,1,\cdots(N^m-1)_+,\quad \nu'=0,1,\cdots,(N^{m'}-1)_+\Big\}.
\end{aligned}\tag{2.13}$$

Similarly we define $\widehat{W}^M_{N,\underline{\eta}^N}((a,b)\times(a',b'))$ as the basis of $L^2((a,b)\times(a',b'))$ obtained starting from $\widehat{W}^M_{N,\underline{\eta}^N}((0,1))$ using the construction shown in (2.12)-(2.13) and we denote with $\widehat{\Upsilon}^M_{j,m,\nu,j',m',\nu',N,\underline{\eta}^N}$ the basis functions of $\widehat{W}^M_{N,\underline{\eta}^N}((a,b)\times(a',b'))$.

3 The use of the wavelet bases in the operator expansion method

To keep the exposition simple we consider obstacles such that $\partial\Omega_1=\partial\Omega$, $\partial\Omega_2=\emptyset$ when $k\neq 0$ so that we consider the problem of solving the boundary value problem (1.1), (1.2), (1.4). Formulae similar to those derived here hold for the remaining cases considered in Section 1.

Let us recall some of the work presented in [1]. Let $\underline{y}=(y_1,y_2,y_3)^T=(y_1,\underline{v}^T)^T$, where $\underline{v}=(y_2,y_3)^T$, be a coordinate system in $\mathbb{R}^3$ (in general a curvilinear coordinate system) and let $\underline{x}=\underline{x}(\underline{y})=\underline{x}((y_1,\underline{v}^T)^T)\in\mathbb{R}^3$, $\underline{y}\in I_1\times I_2\times I_3$ be the change of variables from the $\underline{y}$-coordinates to the canonical cartesian coordinates $\underline{x}$, where $\underline{x}(\underline{y})=(x_1(\underline{y}),x_2(\underline{y}),x_3(\underline{y}))^T$,

$x_i(\underline{y})$, $i=1,2,3$ are given functions and $I_i \subseteq \mathbb{R}$, $i=1,2,3$ are given intervals (not necessarily bounded or open). The spherical, cylindrical and parabolic coordinate systems are examples of changes of variables that satisfy the previous assumptions. We assume that the map $\underline{x}=\underline{x}(\underline{y})$, $\underline{y}\in I_1\times I_2\times I_3$ is sufficiently regular to make sense out of the formulae that follow. Let X be a set contained in an Euclidean space we denote with $\overset{\circ}{X}$ the interior of X.

Let us assume that the obstacle Ω and its boundary $\partial\Omega$ can be represented as follows:

$$\Omega=\{\underline{x}=\underline{x}(\underline{y})=\underline{x}((y_1,\underline{v}^T)^T)\in\mathbb{R}^3\,|\,y_1\in I_1, y_1<\xi(\underline{v}), \underline{v}\in\hat{I}_2\times\hat{I}_3\}, \tag{3.1}$$

$$\partial\Omega=\{\underline{x}=\underline{x}(\underline{y})=\underline{x}((y_1,\underline{v}^T)^T)\in\mathbb{R}^3\,|\,y_1=\xi(\underline{v}), \underline{v}\in\hat{I}_2\times\hat{I}_3\}, \tag{3.2}$$

where $\hat{I}_2$, $\hat{I}_3\subset\mathbb{R}$ are bounded intervals such that $\hat{I}_2\times\hat{I}_3\subseteq I_2\times I_3$, and $\xi(\underline{v})$, $\underline{v}\in\hat{I}_2\times\hat{I}_3$, is a single valued bounded function regular enough to make sense out of the formulae that follow and such that when $\underline{v}\in(\overset{\circ}{\hat{I}_2}\times\overset{\circ}{\hat{I}_3})$ we have $\xi(\underline{v})\in\overset{\circ}{I_1}$. Let

$$\underline{x}_\xi(\underline{v})=\underline{x}((\xi(\underline{v}),\underline{v}^T)^T),\quad \underline{X}_{y_i}(\underline{v})=\frac{\partial\underline{x}_\xi(\underline{v})}{\partial y_i},\quad i=2,3,\quad \underline{v}\in\hat{I}_2\times\hat{I}_3. \tag{3.3}$$

Due to the assumptions made on Ω in Section 1, the surface measure on $\partial\Omega$ is given by:

$$ds_{\partial\Omega}(\underline{v})=\sqrt{g(\underline{v})}\,d\underline{v},\quad \underline{v}\in\hat{I}_2\times\hat{I}_3, \tag{3.4}$$

where $d\underline{v}=dy_2\,dy_3$ is the Lebesgue measure on $\hat{I}_2\times\hat{I}_3$ (see [1] Section 2 for further details) and

$$g(\underline{v})=(\underline{X}_{y_2},\underline{X}_{y_2})(\underline{X}_{y_3},\underline{X}_{y_3})-(\underline{X}_{y_2},\underline{X}_{y_3})(\underline{X}_{y_3},\underline{X}_{y_2}),\quad \underline{v}\in\hat{I}_2\times\hat{I}_3, \tag{3.5}$$

where we remind that in (3.5) the symbol $(\cdot,\cdot)$ denotes the Euclidean scalar product in $\mathbb{R}^3$. Note that the derivatives appearing in (3.3) and as a consequence the function $g(\underline{v})$ defined in (3.5) may be defined only almost everywhere.

Let us introduce now the surface $\partial\Omega_c$, boundary of the set $\Omega_c\subset\mathbb{R}^3$, used in the definition of the single layer potential (1.5) and the auxiliary surface $\partial\Omega_r$, boundary of the set $\Omega_r\subset\mathbb{R}^3$. We remind that the sets Ω_c and Ω_r and their boundaries $\partial\Omega_c$ and $\partial\Omega_r$ must satisfy the following conditions:

i) there exists a surface measure on $\partial\Omega_c$,
ii) $\overline{\Omega_c}\subset\Omega$,
iii) $\overline{\Omega_c}\subset\Omega_r$,
iv) the "distance" between $\partial\Omega_c$ and $\partial\Omega_r$ is "small",
v) the "distance" between $\partial\Omega_r$ and $\partial\Omega$ is "small",
vi) the surfaces $\partial\Omega_c$ and $\partial\Omega_r$ are sufficiently regular to make sense out of the formulae that follow.

Note that $\partial\Omega_r \cap \partial\Omega$ may be non empty so that $v)$ must be interpreted as saying that $\partial\Omega_r$ and $\partial\Omega$ are "close by" surfaces. A similar interpretation must be given to (iv) even if in this case $\partial\Omega_c \cap \partial\Omega_r = \emptyset$. The way in which the series expansion derived below are built will make clear the meaning of the expression "close by".

In [1] it has been shown that we can choose two intervals $\tilde{I}_2 \subset \mathbb{R}$, $\tilde{I}_3 \subset \mathbb{R}$ such that $\tilde{I}_2 \times \tilde{I}_3 \subseteq \hat{I}_2 \times \hat{I}_3$ and that we can define Ω_c and Ω_r to be the following two sets:

$$\Omega_c = \{\underline{x} = \underline{x}(\underline{y}) = \underline{x}((y_1, \underline{v}^T)^T) \in \mathbb{R}^3 \,|\, y_1 \in I_1, y_1 < \xi_c(\underline{v}), \underline{v} \in \tilde{I}_2 \times \tilde{I}_3\}, \tag{3.6}$$

$$\Omega_r = \{\underline{x} = \underline{x}(\underline{y}) = \underline{x}((y_1, \underline{v}^T)^T) \in \mathbb{R}^3 \,|\, y_1 \in I_1, y_1 < \xi_r(\underline{v}), \underline{v} \in \hat{I}_2 \times \hat{I}_3\}, \tag{3.7}$$

so that we have:

$$\partial\Omega_c = \{\underline{x} = \underline{x}(\underline{y}) = \underline{x}((y_1, \underline{v}^T)^T) \in \mathbb{R}^3 \,|\, y_1 = \xi_c(\underline{v}) \in I_1, \underline{v} \in \tilde{I}_2 \times \tilde{I}_3\}, \tag{3.8}$$

$$\partial\Omega_r = \{\underline{x} = \underline{x}(\underline{y}) = \underline{x}((y_1, \underline{v}^T)^T) \in \mathbb{R}^3 \,|\, y_1 = \xi_r(\underline{v}) \in I_1, \underline{v} \in \hat{I}_2 \times \hat{I}_3\}, \tag{3.9}$$

where ξ_c, ξ_r are single valued, bounded, regular functions taking values in $\overset{\circ}{I}_1$ satisfying the following inequalities:

$$\xi(\underline{v}) > \xi_c(\underline{v}), \quad \underline{v} \in \tilde{I}_2 \times \tilde{I}_3, \tag{3.10}$$

$$\xi_r(\underline{v}) > \xi_c(\underline{v}), \quad \underline{v} \in \tilde{I}_2 \times \tilde{I}_3. \tag{3.11}$$

The inequality (3.10) implies that Ω_c is a kind of a "regular" version of Ω made "slimmer" along the coordinate direction y_1.

The regularity of the functions ξ_c, ξ_r will be exploited later when we represent the integral operators resulting from the operator expansion on the wavelet bases built previously. Note that the set defined in (3.8) is a surface and that since ξ_c is a regular function we have that $\partial\Omega_c$ has a surface measure ds given by a formula similar to formula (3.4), that is:

$$ds(\underline{v}) = \sqrt{g_c(\underline{v})}\, d\underline{v}, \quad \underline{v} \in \tilde{I}_2 \times \tilde{I}_3, \tag{3.12}$$

where g_c is given by formula (3.5) when we replace ξ with ξ_c in formula (3.3).

Now we can formulate the operator expansion method.

Let us assume that the assumptions (a) and (b) of Section 1 hold and that formulae (3.2), (3.8), (3.9), (3.12) hold for Ω, Ω_r, and Ω_c and let $\underline{x}_{\xi}(\underline{v})$ be the function defined in (3.3), moreover let $\underline{\phi}_k(\underline{v}) = (1/\imath k)\chi(\underline{x}_{\xi}(\underline{v}))\underline{n}(\underline{x}_{\xi}(\underline{v}))$, $\underline{v} \in \hat{I}_2 \times \hat{I}_3$, and $\underline{x}_{\xi_c}(\underline{v}') = \underline{x}((\xi_c(\underline{v}'), \underline{v}'^T)^T)$, $\underline{v}' = (y_2', y_3')^T \in \tilde{I}_2 \times \tilde{I}_3$, we can rewrite equation (1.7) as follows:

$$\begin{aligned} &\int_{\tilde{I}_2 \times \tilde{I}_3} d\underline{v}' \sqrt{g_c(\underline{v}')} v_k(\underline{x}_{\xi_c}(\underline{v}')) \big\{ \Phi_k(\underline{x}_{\xi}(\underline{v}), \underline{x}_{\xi_c}(\underline{v}')) \\ &\quad + \Big(\underline{\phi}_k(\underline{v}), \nabla_{\underline{x}} \Phi_k(\underline{x}_{\xi}(\underline{v}), \underline{x}_{\xi_c}(\underline{v}')) \Big) \Big\} = g_{1,k}(\underline{x}_{\xi}(\underline{v})), \quad \underline{v} \in \hat{I}_2 \times \hat{I}_3, \end{aligned} \tag{3.13}$$

where $\nabla_{\underline{x}}$ denotes the gradient operator with respect to the variable $\underline{x}$. Remember that since we are assuming $\partial\Omega_2 = \{\emptyset\}$ equation (1.8) should not be considered.

The operator expansion method is based on the idea of taking an expansion of the density v_k in powers of $(\xi-\xi_r)$, regarding v_k as a function of ξ. We use ξ as an independent variable so that, for example, we attribute a meaning to the notation $\mathcal{O}((\xi-\xi_r)^\nu)$, when $\xi\to\xi_r$, $\nu=0,1,\cdots$.

That is we assume that for the density v_k and as a consequence for the single layer potential (1.5) computed in $\underline{x}=\underline{x}_\xi(\underline{v})$ the following expansions hold:

$$v_k(\underline{x}_{\xi_c}(\underline{v}))=\sum_{s=0}^{+\infty}c_{k,s}(\underline{v}),\quad \underline{v}\in\tilde{I}_2\times\tilde{I}_3, \tag{3.14}$$

$$F_k(\underline{x}_\xi(\underline{v}))=\sum_{s=0}^{+\infty}\sum_{\nu=0}^{s}\left\{\frac{(\xi(\underline{v})-\xi_r(\underline{v}))^{s-\nu}}{(s-\nu)!}\right.$$
$$\left.\times\int_{\tilde{I}_2\times\tilde{I}_3}d\underline{v}'\sqrt{g_c(\underline{v}')}\left(\frac{\partial^{s-\nu}\Phi_k}{\partial y_1^{s-\nu}}\right)(\underline{x}_{\xi_r}(\underline{v}),\underline{x}_{\xi_c}(\underline{v}'))c_{k,\nu}(\underline{v}')\right\},\quad \underline{v}\in\hat{I}_2\times\hat{I}_3, \tag{3.15}$$

and

$$c_{k,s}(\underline{v})=\mathcal{O}((\xi(\underline{v})-\xi_r(\underline{v}))^s),\quad \underline{v}\in\tilde{I}_2\times\tilde{I}_3,\quad \xi\to\xi_r,\quad s=0,1,\cdots. \tag{3.16}$$

Note that in equation (3.15) we use a series expansion in powers of $(\xi-\xi_r)$ of the fundamental solution $\Phi_k(\underline{x},\underline{y})$, $\underline{x}=\underline{x}_\xi(\underline{v})\in\partial\Omega$, $\underline{v}\in\hat{I}_2\times\hat{I}_3$, $\underline{y}\in\partial\Omega_c$. Thank to these expansions we solve the integral equation (3.13) using a perturbative series, that is in (3.13) we use an expansion in powers of $(\xi-\xi_r)$ of the unknown density (i.e., (3.14), (3.16)) and of the integral kernel.

Let K_{ξ_r,ξ_c} be the following integral kernel: for $\underline{v}\in\hat{I}_2\times\hat{I}_3$, $\underline{v}'\in\tilde{I}_2\times\tilde{I}_3$,

$$K_{\xi_r,\xi_c}(\underline{v},\underline{v}')=\sqrt{g_c(\underline{v}')}\left[\Phi_k(\underline{x}_{\xi_r}(\underline{v}),\underline{x}_{\xi_c}(\underline{v}'))+\left(\underline{\phi}_k(\underline{v}),(\nabla_{\underline{x}}\Phi_k)(\underline{x}_{\xi_r}(\underline{v}),\underline{x}_{\xi_c}(\underline{v}'))\right)\right]. \tag{3.17}$$

We can formulate the operator expansion method as follows:

Lemma 3.1. *Let $\partial\Omega_1=\partial\Omega$, $\partial\Omega_2=\emptyset$, and let k,Ω_r, Ω_c, $K_{\xi_r,\xi_c}(\underline{v},\underline{v}')$, $\underline{v}\in\hat{I}_2\times\hat{I}_3$, $\underline{v}'\in\tilde{I}_2\times\tilde{I}_3$ be as above. We assume that the solution of* (1.1), (1.2), (1.4) *is given by the single layer potential F_k defined in* (1.5) *and the validity of the series expansion* (3.14), (3.16) *for the corresponding density function $v_k(\underline{y})$, $\underline{y}\in\partial\Omega_c$. Then the coefficients $c_{k,s}(\underline{v})$, $\underline{v}\in\tilde{I}_2\times\tilde{I}_3$, of the expansion* (3.14) *are the solutions of the following integral equations:*

$$\int_{\tilde{I}_2\times\tilde{I}_3}d\underline{v}'c_{k,s}(\underline{v}')K_{\xi_r,\xi_c}(\underline{v},\underline{v}')=d_{k,s}(\underline{v}),\quad \underline{v}\in\hat{I}_2\times\hat{I}_3,\quad s=0,1,2,\cdots, \tag{3.18}$$

where

$$d_{k,0}(\underline{v})=g_{1,k}(\underline{x}_\xi(\underline{v})),\qquad \underline{v}\in\hat{I}_2\times\hat{I}_3, \tag{3.19}$$

$$d_{k,s}(\underline{v})=\sum_{\nu=0}^{s-1}\frac{(\xi(\underline{v})-\xi_r(\underline{v}))^{s-\nu}}{(s-\nu)!}\int_{\tilde{I}_2\times\tilde{I}_3}d\underline{v}'\sqrt{g_c(\underline{v}')}c_{k,\nu}(\underline{v}')$$
$$\times\left\{\left(\underline{\phi}_k(\underline{v}),\left(\frac{\partial^{s-\nu}}{\partial y_1^{s-\nu}}(\nabla_{\underline{x}}\Phi_k)\right)\ (\underline{x}_{\xi_r}(\underline{v}),\underline{x}_{\xi_c}(\underline{v}'))\right)+\left(\frac{\partial^{s-\nu}}{\partial y_1^{s-\nu}}\Phi_k\right)(\underline{x}_{\xi_r}(\underline{v}),\underline{x}_{\xi_c}(\underline{v}'))\right\},$$
$$\underline{v}\in\hat{I}_2\times\hat{I}_3,\ s=1,2,\cdots. \tag{3.20}$$

Proof. See [1] Lemma 2.1. □

Finally as shown in [1] Lemma 2.3 we can write the solution of the exterior boundary value problem (1.1), (1.2), (1.4) as follows:

$$u_k^s(\underline{x}) = u_{k,S}^s(\underline{x}) + R_{k,S}(\underline{x}), \qquad \underline{x} \in \mathbb{R}^3 \setminus \overline{\Omega}, \tag{3.21}$$

where

$$u_{k,S}^s(\underline{x}) = \int_{\tilde{I}_2 \times \tilde{I}_3} d\underline{v}' \sqrt{g_c(\underline{v}')} \Phi_k(\underline{x}, \underline{x}_{\xi_c}(\underline{v}')) \sum_{\nu=0}^{S} c_{k,\nu}(\underline{v}'), \quad \underline{x} \in \mathbb{R}^3 \setminus \overline{\Omega}, \tag{3.22}$$

and $R_{k,S}(\underline{x}) = o((\xi - \xi_r)^S)$ when $\xi \to \xi_r$.

Let us solve the integral equations (3.18) in the appropriate L^2 space using the new wavelet bases introduced in Section 2. Without loss of generality, to keep the exposition simple, in the following we assume that $\tilde{I}_2 \times \tilde{I}_3 = \hat{I}_2 \times \hat{I}_3$. In fact with a change of variables the integral equation (3.18) over $\tilde{I}_2 \times \tilde{I}_3$ can be transformed into an integral equation over the set $\hat{I}_2 \times \hat{I}_3$.

Let $N = 2$ and $W_{N,\underline{\eta}^N}^M(\hat{I}_2 \times \hat{I}_3)$ be the wavelet basis of $L^2(\hat{I}_2 \times \hat{I}_3)$ defined in (2.13), for $m = 0,1,\cdots$ let $I_{M,N,m}$ be the following set of indices:

$$I_{M,N,m} = \left\{ \underline{\mu} = (j, \hat{m}, \nu)^T \,\middle|\, -M \le j \le M-1;\ \hat{m} = \begin{cases} m, & j \ge 0 \\ 0, & j < 0 \end{cases};\ 0 \le \nu \le (N^{\hat{m}} - 1)_+ \right\}. \tag{3.23}$$

We represent the unknowns of the integral equations (3.18) $c_{k,s}$, $s = 0,1,\cdots$, on the basis $W_{N,\underline{\eta}^N}^M(\hat{I}_2 \times \hat{I}_3)$:

$$c_{k,s}(\underline{v}) = \sum_{m=0}^{+\infty} \sum_{\underline{\mu} \in I_{M,N,m}} \sum_{m'=0}^{+\infty} \sum_{\underline{\mu}' \in I_{M,N,m'}} c_{k,s,\underline{\mu},\underline{\mu}'} \Upsilon_{\underline{\mu},\underline{\mu}',N,\underline{\eta}^N}^M(\underline{v}), \quad \underline{v} \in \hat{I}_2 \times \hat{I}_3. \tag{3.24}$$

Similarly we represent the data $d_{k,s}$, $s = 0,1,\cdots$, of the integral equations (3.18):

$$d_{k,s}(\underline{v}) = \sum_{m=0}^{+\infty} \sum_{\underline{\mu} \in I_{M,N,m}} \sum_{m'=0}^{+\infty} \sum_{\underline{\mu}' \in I_{M,N,m'}} d_{k,s,\underline{\mu},\underline{\mu}'} \Upsilon_{\underline{\mu},\underline{\mu}',N,\underline{\eta}^N}^M(\underline{v}), \quad \underline{v} \in \hat{I}_2 \times \hat{I}_3. \tag{3.25}$$

Note that when $\underline{\mu} \in I_{M,N,m}$ and $\underline{\mu}' \in I_{M,N,m'}$ the function $\Upsilon_{\underline{\mu},\underline{\mu}',N,\underline{\eta}^N}^M$ is uniquely determined by its indices. In fact when $m \neq m'$ $I_{M,N,m} \cap I_{M,N,m'} = \emptyset$. Furthermore we note that $W_{N,\underline{\eta}^N}^M(\hat{I}_2 \times \hat{I}_3)$ is a basis made of real functions that we use to expand complex functions. This corresponds to expand the real and the imaginary part of the complex functions considered simultaneously on the wavelet basis. Hence in general the coefficients $c_{k,s,\underline{\mu},\underline{\mu}'}$ and $d_{k,s,\underline{\mu},\underline{\mu}'}$ of the wavelet expansions (3.24) and (3.25) are complex numbers.

Finally using the tensor product basis we have the following representation for the integral kernel K_{ξ_r,ξ_c}:

$$K_{\xi_r,\xi_c}(\underline{v},\underline{v}')=\sum_{n=0}^{+\infty}\sum_{\underline{\mu}\in I_{M,N,n}}\sum_{n'=0}^{+\infty}\sum_{\underline{\mu}'\in I_{M,N,n'}}\Upsilon^{M}_{\underline{\mu},\underline{\mu}',N,\underline{\eta}^N}(\underline{v})$$
$$\times\sum_{m=0}^{+\infty}\sum_{\underline{\tilde{\mu}}\in I_{M,N,m}}\sum_{m'=0}^{+\infty}\sum_{\underline{\tilde{\mu}}'\in I_{M,N,m'}}a_{k,s,\underline{\mu},\underline{\mu}',\underline{\tilde{\mu}},\underline{\tilde{\mu}}'}\Upsilon^{M}_{\underline{\tilde{\mu}},\underline{\tilde{\mu}}',N,\underline{\eta}^N}(\underline{v}'),\quad \underline{v},\underline{v}'\in\hat{I}_2\times\hat{I}_3. \tag{3.26}$$

Note that K_{ξ_r,ξ_c} is a complex valued kernel whose real and imaginary parts are expanded on a basis of real functions.

Let m^* be a positive integer and let $J_{M,N,m^*}=M^2(N^{m^*+1}+N-2)^2/\,(N-1)^2$, truncating the series (3.24) and (3.25) when $m=m'=m^*$ and the series (3.26) when $m=m'=n=n'=m^*$ we approximate the sequence of integral equations (3.18)-(3.20) with the following sequence of (complex) systems of linear equations:

$$A^{k,M}\underline{c}^{k,s,M}=\underline{d}^{k,s,M},\quad s=0,1,\cdots, \tag{3.27}$$

where $\underline{c}^{k,s,M}$, $\underline{d}^{k,s,M}\in\mathbf{C}^{J_{M,N,m^*}}$, are the finite dimensional vectors whose components are respectively an approximation of the first J_{M,N,m^*} coefficients of the wavelet expansion of the unknowns $c_{k,s}$, and the first J_{M,N,m^*} coefficients of the wavelet expansion of the data $d_{k,s}$, given in (3.24) and (3.25) respectively ordered by columns. More precisely, for $s=0,1,\cdots$, we have:

$$\underline{c}^{k,s,M}=\begin{pmatrix} c^{k,s,M}_1\approx c_{k,s,(-M,0,0)^T,(-M,0,0)^T}\\ c^{k,s,M}_2\approx c_{k,s,(-M,0,0)^T,(-M+1,0,0)^T}\\ \vdots\\ c^{k,s,M}_M\approx c_{k,s,(-M,0,0)^T,(-1,0,0)^T}\\ c^{k,s,M}_{M+1}\approx c_{k,s,(-M,0,0)^T,(0,0,0)^T}\\ c^{k,s,M}_{M+2}\approx c_{k,s,(-M,0,0)^T,(0,1,0)^T}\\ c^{k,s,M}_{M+3}\approx c_{k,s,(-M,0,0)^T,(0,1,1)^T}\\ \vdots\\ c^{k,s,M}_{M+\frac{N^{m^*+1}-1}{N-1}}\approx c_{k,s,(-M,0,0)^T,(0,m^*,N^{m^*}-1)^T}\\ \vdots\\ c^{k,s,M}_{J_{M,N,m^*}}\approx c_{k,s,(M-1,m^*,N^{m^*}-1)^T,(M-1,m^*,N^{m^*}-1)^T} \end{pmatrix}, \tag{3.28}$$

and a similar formula holds for $\underline{d}^{k,s,M}$ when we replace $c^{k,s,M}_i$ with $d^{k,s,M}_i$, $i=1,2,\cdots,J_{M,N,m^*}$, $c_{k,s,\underline{\mu},\underline{\mu}'}$ with $d_{k,s,\underline{\mu},\underline{\mu}'}$, $\underline{\mu}$, $\underline{\mu}'\in I_{M,N,m}$, $m=0,1,\cdots,m^*$ and $\approx$ with $=$. The entries $A^{k,M}_{i,j}$ of the matrix $A^{k,M}\in\mathbf{C}^{J_{M,N,m^*}\times J_{M,N,m^*}}$ are the coefficients $a_{k,s,\underline{\mu},\underline{\mu}',\underline{\tilde{\mu}},\underline{\tilde{\mu}}'}$ of formula (3.26) when $\underline{\mu}\in I_{M,N,n}$, $n=0,1,\cdots,m^*$, $\underline{\mu}'\in I_{M,N,n'}$, $n'=0,1,\cdots,m^*$, $\underline{\tilde{\mu}}\in I_{M,N,m}$, $m=0,1,\cdots,m^*$, $\underline{\tilde{\mu}}'\in I_{M,N,m'}$,

$m'=0,1,\cdots,m^*$. The ordering of the entries of the matrix $A^{k,M}$ is induced by (3.27) and by the ordering of the elements of the vectors $\underline{c}^{k,s,M}$ and $\underline{d}^{k,s,M}$ defined in (3.28). Let $\tau>0$ be a threshold. We define the "sparse" version of $A^{k,M}$ corresponding to the threshold τ as the matrix $A^{k,M,\tau}\in\mathbf{C}^{J_{M,N,m^*}\times J_{M,N,m^*}}$ whose entries are given by:

$$A_{i,j}^{k,M,\tau}=\begin{cases} A_{i,j}^{k,M}, & \text{if } |A_{i,j}^{k,M}|>\tau, \\ 0, & \text{if } |A_{i,j}^{k,M}|\leq\tau, \end{cases} \quad i,j=1,2,\cdots,J_{M,N,m^*}. \tag{3.29}$$

We want to approximate the linear system (3.27) by replacing the matrix $A^{k,M}$ with its truncated version $A^{k,M,\tau}$.

Note that the matrix $A^{k,M}$ is a generic matrix, possibly a dense matrix, however when m^* increases we expect the matrix $A^{k,M,\tau}$ to be a sparse matrix even for small values of the threshold $\tau>0$. This expectation is based on Lemma A.2. The use of the approximating (sparse) matrix $A^{k,M,\tau}$ rather than $A^{k,M}$ makes possible to work in high dimensional spaces at an affordable computational cost. For $\underline{y}=(y_1,y_2,\cdots,y_{J_{M,N,m^*}})^T\in\mathbf{C}^{J_{M,N,m^*}}$ we denote with $\|\underline{y}\|_\infty=\max_{1\leq i\leq J_{M,N,m^*}}|y_i|$ the infinity norm of the vector $\underline{y}$ and for $A\in\mathbf{C}^{J_{M,N,m^*}\times J_{M,N,m^*}}$ we denote with $\|A\|_\infty$ the induced matrix norm. We have:

Theorem 3.1. *Let $k\neq 0$, $\partial\Omega_1=\partial\Omega$, $\partial\Omega_2=\emptyset$, and Ω_c, Ω_r be as above. Let $M\geq 1$ be a given integer. We assume that $\partial\Omega_r$ and $\partial\Omega_c$ are $(M+2)$-times continuously differentiable surfaces, that problem* (1.1), (1.2), (1.4) *has a unique solution that can be extended to $\mathbb{R}^3\setminus\overline{\Omega}_c$, and that this solution can be represented by the single layer potential* (1.5) *with a density function v_k defined on $\partial\Omega_c$. Moreover, we assume that $-k^2$ is not an eigenvalue of the Laplace operator in Ω_c equipped with the homogeneous boundary condition* (1.2) *on $\partial\Omega_c$. Finally, let m^* be a non-negative integer, $\tau>0$ be a threshold, let $A^{k,M}\in\mathbf{C}^{J_{M,N,m^*}\times J_{M,N,m^*}}$ and $A^{k,M,\tau}\in\mathbf{C}^{J_{M,N,m^*}\times J_{M,N,m^*}}$ be the matrices given in* (3.27) *and* (3.29) *respectively. Then for m^* large enough $A^{k,M}$ is a non-singular matrix, and when τ is chosen such that*

$$0<\tau<\frac{\delta\|(A^{k,M})^{-1}\|_\infty^{-1}}{J_{M,N,m^*}}, \tag{3.30}$$

for some $0<\delta<1$, then the matrix $A^{k,M,\tau}$ is also non singular. Moreover, we have:

$$\|A^{k,M}-A^{k,M,\tau}\|_\infty\leq\delta\|(A^{k,M})^{-1}\|_\infty^{-1}, \tag{3.31}$$

$$\|(A^{k,M,\tau})^{-1}\|_\infty\leq\frac{\|(A^{k,M})^{-1}\|_\infty}{(1-\delta)}. \tag{3.32}$$

Let $\underline{c}^{k,s,M}$ be the solution of the linear systems (3.27) *and $\underline{c}^{k,s,M,\tau}$ be the solution of the "sparse" linear systems:*

$$A^{k,M,\tau}\underline{c}^{k,s,M,\tau}=\underline{d}^{k,s,M},\quad s=0,1,\cdots. \tag{3.33}$$

Then we have

$$\|\underline{c}^{k,s,M}-\underline{c}^{k,s,M,\tau}\|_\infty\leq\frac{\delta}{1-\delta}\|\underline{c}^{k,s,M}\|_\infty,\quad s=0,1,\cdots. \tag{3.34}$$

Finally let $a_{k,s,\underline{\mu},\underline{\mu}',\underline{\tilde{\mu}},\underline{\tilde{\mu}}'}$, *be the entries of the matrix* $A^{k,M}$ *defined in* (3.26) *where* $\underline{\mu}=(j,\hat{m},\nu)^T$, $\underline{\mu}'=(j',\hat{m}',\nu')^T$, $\underline{\tilde{\mu}}=(\tilde{j},\tilde{m},\tilde{\nu})^T$, $\underline{\tilde{\mu}}'=(\tilde{j}',\tilde{m}',\tilde{\nu}')^T$, *and let* $K_{\xi_r,\xi_c}\in C^M(\overline{\hat{I}_2\times\hat{I}_3}\times\overline{\tilde{I}_2\times\tilde{I}_3})$. *Then for* $|k|>k_{min}>0$, *there exists a positive constant* D'_M *independent of* k *and* N *such that the entries of the matrix* $A^{k,M}$ *whose indices satisfy the inequality:*

$$\left(N^{\max(\hat{m},\hat{m}',\tilde{m},\tilde{m}')}\right)^{M+1}\geq|k|^{M+1}D'_M/\tau, \tag{3.35}$$

are smaller than τ *in absolute value. That is we have:*

$$|a_{k,s,\underline{\mu},\underline{\mu}',\underline{\tilde{\mu}},\underline{\tilde{\mu}}'}|\leq|k|^{M+1}D'_M\frac{1}{\left(N^{\max(\hat{m},\hat{m}',\tilde{m},\tilde{m}')}\right)^{M+1}}. \tag{3.36}$$

Proof. It follows from Theorem A.1 that the proof that the matrix $A^{k,M}$ is non singular and the proofs for (3.31), (3.32), (3.34) are analogous to the proofs in Lemma 3.1 of [1]. The proof of (3.35) follows from Lemma A.2 since $\partial\Omega_c$ and $\partial\Omega_r$ are surfaces sufficiently regular to guarantee that $K_{\xi_r,\xi_c}\in C^M(\overline{\hat{I}_2\times\hat{I}_3}\times\overline{\tilde{I}_2\times\tilde{I}_3})$ and $|k|^{M+1}D'_M$ is a positive constant that is an upper bound of the sum of the absolute values of the M-th order derivatives of the kernel $K_{\xi_r,\xi_c}(\underline{v},\underline{v}')$ with respect to the components of $\underline{v}\in\overline{\hat{I}_2\times\hat{I}_3}$ and $\underline{v}'\in\overline{\tilde{I}_2\times\tilde{I}_3}$. This concludes the proof. □

Eqs. (3.35)-(3.36) show that when the constant $|k|^{M+1}D'_M$ remains bounded as a function of M (when M goes to infinity) we have that when the number of vanishing moments M increases the number of the entries of the matrix $A^{k,M}$ guaranteed to be less than the threshold τ and the percentage of the entries of the matrix $A^{k,M}$ guaranteed to be less than the threshold τ increase. The same happens when we fix M and increase N (see (3.36)). This last choice is very efficient when the constant $|k|^{M+1}D'_M$ is not bounded when M goes to infinity.

We note that the results contained in formulae (3.31)-(3.34) hold under the weaker assumptions that $\partial\Omega_c$ is a twice continuously differentiable surface and $\partial\Omega_r$ is a Lipschitz surface.

We conclude this section by reconsidering formula (1.16) for the approximation of the solution $u^s(\underline{x},t)$ of the time dependent scattering problem (1.9)-(1.15). Formula (1.16) is based on the assumption that the incoming wave $u^i(\underline{x},t)$ satisfies the wave equation with wave propagation velocity $c>0$ in $\mathbb{R}^3\times\mathbb{R}$. In fact this assumption implies the following representation formula for u^i:

$$u^i(\underline{x},t)=\frac{1}{(2\pi)^4}\int_{\mathbb{R}}d\omega w(\omega)e^{-\imath\omega t}\int_{\partial B}ds_{\partial B}(\underline{\alpha})W(\omega,\underline{\alpha})e^{\imath\frac{\omega}{c}(\underline{\alpha},\underline{x})},\quad(\underline{x},t)\in\mathbb{R}^3\times\mathbb{R}, \tag{3.37}$$

where $ds_{\partial B}(\underline{\alpha})$ is the surface measure on ∂B, $w(\omega)$, $\omega\in\mathbb{R}$ is a given positive function that plays the role of a weight function and $W(\omega,\underline{\alpha})$, $(\omega,\underline{\alpha})\in\mathbb{R}\times\partial B$ is a suitable distribution. Formula (3.37) suggests the following representation formula for u^s:

$$u^s(\underline{x},t)=\frac{1}{(2\pi)^4}\int_{\mathbb{R}}d\omega w(\omega)e^{-\imath\omega t}\int_{\partial B}ds_{\partial B}(\underline{\alpha})W(\omega,\underline{\alpha})u^s_{\frac{\omega}{c},\underline{\alpha}}(\underline{x}),\quad(\underline{x},t)\in(\mathbb{R}^3\setminus\overline{\Omega})\times\mathbb{R}, \tag{3.38}$$

where $u^s_{\frac{\omega}{c},\underline{\alpha}}(\underline{x})$, $\underline{x}\in\mathbb{R}^3\setminus\overline{\Omega}$, $(\omega,\underline{\alpha})\in\mathbb{R}\times\partial B$ are functions to be determined. Note that formulae (3.37), (3.38) depend only on the product $w(\omega)W(\omega,\underline{\alpha})$ and not on the individual factors $w(\omega)$ and $W(\omega,\underline{\alpha})$.

It is easy to see that formula (1.16) is obtained approximating (3.38) with a numerical quadrature rule.

Finally we make a rough comparison between the computational cost of the algorithm proposed in this section and the computational cost of the fast multipole algorithms [3–5]. Let N_S be the number of elements used to decompose the obstacle surface (spatial samples) and N_t be the number of time steps in the time domain (see [3]). These two numbers considered in the fast multipole algorithms can be associated with the numbers J_{M,N,m^*} and N_1N_2 respectively of the algorithm proposed in this section, where J_{M,N,m^*} is the number of the elements of the wavelet series expansion used to represent the unknown density and due to formula (1.16) N_1N_2 corresponds to N_t. This last correspondence is very rough, in fact in the method proposed here once computed the N_1N_2 terms $u^s_{\omega_i/c,\underline{\alpha}_j}$, $i=1,\cdots,N_1$, $j=1,\cdots,N_2$ on a spatial grid, the cost of evaluating $u^s(\underline{x},t)$ for several values of t consists only in re-summing the terms $e^{-\imath\omega_i t}u^s_{\omega_i/c,\underline{\alpha}_j}$. Furthermore, thank to the wavelet basis used (see Lemma A.1) the computational cost of the solution of the linear systems (3.29) is $\mathcal{O}(J^2_{M,N,m^*})$ as $J_{M,N,m^*}\to+\infty$. Hence we can conclude that using the analogy suggested above the computational cost of the algorithm proposed in this section is linear in the number of the time steps and quadratic in the number of the spatial samples compared to the fast multipole methods that require $\mathcal{O}(N_s^{3/2+1/4})$ as $N_s\to+\infty$ to compute the matrix elements and then $\mathcal{O}(N_s^{3/2})$, as $N_s\to+\infty$, to complete the computation, where N_s is the number of the spatial samples (see, e.g., [4]). Note that, in the algorithm considered in this section due to the parallel implementation of the algorithm proposed, the computational cost to solve the linear system (3.29) is $\mathcal{O}(J^2_{M,N,m^*}/n_p)$ as $J_{M,N,m^*}\to+\infty$ where n_p is the number of processors used.

4 Numerical results

We present four numerical experiments. The first two experiments show the convergence of the series expansion (3.14) computed with the numerical method presented in Section 3 involving the truncation procedure associated with the threshold parameter $\tau>0$ and the validity of formula (1.5). Moreover, in the first experiment we study the parallel performance of the numerical method proposed. The last two experiments are qualitative and they show in colour figures (see Figs. 3 and 4) the scattering from two realistic obstacles, that is the simplified versions of a submarine and of the NASA space shuttle shown in Fig. 1(b) and Fig. 2(b) respectively, when hit by an incoming wave packet.

The curvilinear coordinate systems used in the experiments are the spherical coordinate system and the cylindrical coordinate system. The algorithm described in Section 3 has been coded in Fortran 77 and tested on the computing grid of Enea (Roma, Italy). The ENEA grid is made of computers located in 12 research centers around Italy.

We use this computing infrastructure both as a grid and as a parallel machine (i.e. MIMD machine). In fact the computation of the solution of the time harmonic problems (1.1)-(1.4) needed to solve the time dependent scattering problem (1.9)-(1.15) has been carried out in two steps. The first step, the computation of the matrix $A^{k,M,\tau}$, has been carried out using the infrastructure as a grid, that is N_p asynchronous programs are executed. When the number of (real) unknowns involved in the problem is approximately $5\cdot10^5$ (i.e. $J_{M,N,m^*}\approx 2.5\cdot10^5$) we use $N_p=512$ asynchronous programs, that is we run 512 executable programs and each one of these programs computes $J_{M,N,m^*}/N_p$ rows of the matrix $A^{k,M,\tau}$. Note that in our experiments $J_{M,N,m^*}/N_p$ is an integer. The second step, the computation of the solution of the linear systems (3.33) for fixed k (one system for each order of the perturbation series considered) and the remaining parts of the computation is done with a parallel code implemented using multiple instructions multiple data programming mode (MIMD) and using MPI as message passing library and is executed on one of the MIMD machines contained in the grid.

The wavelet basis used in the numerical experiments has been obtained using the symbolic Matlab package to implement the procedure described in Section 2. The functions $\widehat{\Psi}^M_{j,N,\eta^N}$, $j=0,1,\cdots,M-1$, i.e., the solution of (2.6), (2.7), (2.10), when $M=2$, $N=2$ and $\eta_1=1/2$ are:

$$\widehat{\Psi}^2_{0,2,1/2}=\begin{cases} -1+6x, & 0<x<\frac{1}{2},\\ -5+6x, & \frac{1}{2}\le x<1,\end{cases}\qquad \widehat{\Psi}^2_{1,2,1/2}=\begin{cases} \sqrt{3}(1-4x), & 0<x<\frac{1}{2},\\ \sqrt{3}(-3+4x), & \frac{1}{2}\le x<1.\end{cases} \tag{4.1}$$

In the numerical experiments that follow we always use the bases generated through the multiresolution procedure and the tensor product starting from the functions $\widehat{\Psi}^2_{j,2,1/2}$, $j=0,1$ given in (4.1). In this section, we denote with $u^s_{k,S,m^*,\tau}$ the solution of problem (1.1)-(1.4) obtained with the expansion (3.14) truncated at order $s=S$ when the coefficients of the series expansion are approximated with the solution of the linear systems (3.33). We have $J_{2,2,m^*}=2^{2(m^*+1)}$ so that in these circumstances the coefficients matrices of the linear systems (3.33) are matrices of (complex) dimension $2^{2(m^*+2)}\times 2^{2(m^*+2)}$. Remind that the functions $\widehat{\Psi}^2_{j,2,1/2}$, $j=0,1$ given in (4.1) are not uniquely determined by (2.6)-(2.7). We have made some experiments using "wavelet mother functions" solutions of (2.6)-(2.7) with $M=1$, $N=2$, $\eta_1=1/2$ (i.e., the Haar's basis) and with $M=2$, $N=2$, $\eta_1=1/2$ different from the functions (4.1). The choice of (4.1) as "wavelet mother functions" is justified by the facts that this choice gives satisfactory "compression factors" and that the coefficients of the polynomials appearing in (4.1) are expressed by simple formulae.

Example 4.1. The first experiment consists in the time harmonic scattering phenomenon generated by a plane wave impinging on an acoustically soft sphere (i.e.: $\chi(\underline{x})=0$, $\underline{x}\in\partial\Omega$) of radius one and center the origin. The incoming wave has been chosen equal to $u^i(\underline{x},t)=e^{-\imath\omega^* t}e^{\imath(\omega^*/c)(\underline{\alpha}^*,\underline{x})}$, where $\underline{\alpha}^*=(\sin\theta\cos\phi,\sin\theta\sin\phi,\cos\theta)^T$, $\theta=\pi$, $\phi=0$ and $\omega^*=1$ and we have chosen $c=1$. In this experiment we have $R_T=1/\pi$.

The solution of this problem is given by a series of spherical harmonics (see, e.g., [29,

p. 24]):

$$u^s(\underline{x}) = -4\pi \sum_{l=0}^{+\infty} \frac{i^l j_l(\omega^*) h_l^{(1)}(\omega^* \|\underline{x}\|)}{h_l^{(1)}(\omega^*)} \sum_{m=-l}^{l} Y_l^m(\hat{\underline{x}}) Y_l^m(\underline{\alpha}^*), \quad \underline{x} = \|\underline{x}\| \hat{\underline{x}}, \quad \hat{\underline{x}} \in \partial B, \tag{4.2}$$

where $\|\underline{x}\| > 1$, and $h_l^{(1)}(z)$, $j_l(z)$ are the spherical Hankel and Bessel functions of index l respectively, and $Y_l^m(\hat{\underline{x}})$ are the spherical harmonics.

Note that in this experiment, we have used the spherical coordinate system to build expansion (3.14) and that we have chosen $\hat{I}_2 \times \hat{I}_3 = \tilde{I}_2 \times \tilde{I}_3 = [0,\pi] \times (0,2\pi]$, $\xi_r(\underline{v}) = 1$, $\underline{v} \in \hat{I}_2 \times \hat{I}_3$ and $\xi_c(\underline{v}) = 0.9$, $\underline{v} \in \tilde{I}_2 \times \tilde{I}_3$.

We compare $u^s_{\omega^*,S,m^*,\tau}$ obtained with the numerical method of Section 3 with $u^s_{L^*}$ obtained by truncating the expansion (4.2) at $l = L^*$ and we choose $L^* = 10$. Let

$$\underline{x}^*_{i,j} = \left(1.5\sin\left(\frac{i\pi}{20}\right)\cos\left(\frac{j\pi}{10}\right), 1.5\sin\left(\frac{i\pi}{20}\right)\sin\left(\frac{j\pi}{10}\right), 1.5\cos\left(\frac{i\pi}{20}\right)\right)^T, \tag{4.3}$$

for $1 \le i \le 19$, $0 \le j \le 20$, $(i,j) = (0,1)$, and $(i,j) = (20,1)$. Let

$$\varepsilon_S^{m^*,\tau} = \frac{1}{\lambda} \sqrt{\sum_{i=0}^{20} \left| u^s_{\omega^*,S,m^*,\tau}(\underline{x}^*_{i,1}) - u^s_{L^*}(\underline{x}^*_{i,1}) \right|^2 + \sum_{i=1}^{19} \sum_{j=0}^{20} \left| u^s_{\omega^*,S,m^*,\tau}(\underline{x}^*_{i,j}) - u^s_{L^*}(\underline{x}^*_{i,j}) \right|^2}, \tag{4.4}$$

where $\lambda = \sqrt{\sum_{i=0}^{20} \left| u^s_{L^*}(\underline{x}^*_{i,1}) \right|^2 + \sum_{i=1}^{19} \sum_{j=0}^{20} \left| u^s_{L^*}(\underline{x}^*_{20,1}) \right|^2}$.

Let $B_{1.5} = \{\underline{x} \in \mathbb{R}^3 \,|\, \|\underline{x}\| < 1.5\}$. We note that $\underline{x}^*_{i,j} \in \partial B_{1.5}$ and that the approximate solution $u^s_{L^*}$ when $L^* = 10$ on $\partial B_{1.5}$ has 4-6 significant digits correct. Table 1 shows that when $S = 0$ the behavior of $\varepsilon_S^{m^*,\tau}$ as a function of the (complex) dimension $J_{2,2,m^*} = 2^{2(m^*+2)}$ of the linear system solved to approximate the integral equations and of the threshold τ used in the truncation procedure. In the last two columns of Table 1 we show the compression factor C_{comp}, that is the fraction of the entries of the matrix $A^{k,M}$ (see (3.27)) that have been set to zero by the truncation procedure (see (3.33)) (i.e. C_{comp} times the number of entries of $A^{k,M}$ is equal to the number of entries set to zero), and the parameter E^τ that is defined as follows:

$$E^\tau = \tau \frac{2^{2(m^*+2)}(1 - C_{comp})}{\|A^{k,M}\|_F}, \tag{4.5}$$

where $\|*\|_F$ is the Frobenius norm of the matrix $*$. For example,

$$\|A^{k,M}\|_F = \sqrt{\sum_{i=1}^{2^{2(m^*+2)}} \sum_{j=1}^{2^{2(m^*+2)}} |A^{k,M}_{i,j}|^2}.$$

Note that we have:

$$\frac{\|A^{k,M} - A^{k,M,\tau}\|_F}{\|A^{k,M}\|_F} \le E^\tau. \tag{4.6}$$

Table 1: Example 4.1: The behavior of $\varepsilon_S^{m^*,\tau}$, C_{comp}, E^τ when $S=0$.

m^*	$2^{2(m^*+2)}$	τ	$\varepsilon_S^{m^*,\tau}$	C_{comp}	E^τ
2	256	0	7.40e-02	0	0
3	1024	0	1.67e-02	0	0
4	4096	0	5.77e-03	0	0
5	16384	1.0e-08	3.85e-04	0.82	9.20e-06
6	65536	2.1e-07	3.83e-04	0.95	5.77e-05
7	262144	4.2e-06	3.79e-04	0.99	6.99e-05

Table 2: Example 4.1: Execution time versus number of processors.

processors	execution time	processors	execution time
2	309.16s	16	47.75s
4	155.83s	32	31.58s
8	83.85s		

Table 1 shows that when the number $2^{2(m^*+2)}$ of the (complex) unknowns increases the accuracy in the numerical approximation increases until the number of (complex) unknowns reaches 16384, since then it remains substantially unchanged. This is due to the fact that the error $\varepsilon_S^{m^*,\tau}$ observed comes from the quadrature rule used to compute the coefficients of the wavelet expansion of the integral kernel and from the fact that the truncation procedure, used when $2^{2(m^*+2)}>4096$, guarantees five digits of accuracy when the solution of (3.27) is approximated with the solution of (3.33). Moreover, in Table 1 we can see that also when the compression factors are large, the quantity E^τ is small. This implies that the sparse version $A^{k,M,\tau}$ of $A^{k,M}$ is a satisfactory approximation of the matrix $A^{k,M}$.

Table 2 shows the performance of the second step of the algorithm proposed in Section 3 when parallel computing on a MIMD machine (i.e.: SP4 machine) is employed. We consider the previous numerical experiment when the number of the (complex) unknowns is 4096, that is when $m^*=4$. The execution time is measured using the (Fortran) MPI routine $MPI\_WTIME()$ that gives a floating point number representing in seconds the elapsed wall clock time. Note that the speed up factor going from 2 to 8 processors is 0.92. In fact passing from 2 to 8 processors, the execution time is divided by 3.68 so that the speed up factor is the ratio $3.68/4\approx 0.92$. Passing from 2 to 16 processors the speed up factor is 0.81 and finally passing from 2 to 32 is 0.61. Note that the computational cost of the algorithm proposed when the number of unknowns used is large is essentially due to the cost of the first step, that is the cost of computing the entries of the matrix $A^{k,M}$. The computational cost of the second step becomes negligible when the number of the unknowns used increases.

Example 4.2. The second experiment consists in the time harmonic scattering phenomenon generated by an acoustically soft double cone (i.e.: $\chi(\underline{x})=0$, $\underline{x}\in\partial\Omega$) when hit by a time harmonic plane wave $u^i(\underline{x},t)=e^{-\imath\omega^* t}u^i_{\omega^*}(\underline{x})=e^{-\imath\omega^* t}e^{\imath k^* x_3}$, where $k^*=(\omega^*/c)$ is the wave number. The double cone is an obstacle that can be easily represented in the cylindrical coordinate system (r_1,ϕ,x_3) by the following formulae:

$$\Omega=\{\underline{x}=(r_1\cos(\phi),r_1\sin(\phi),x_3)^T, 0\le r_1<\xi(x_3),\ (\phi,x_3)\in[0,2\pi)\times[-z^*,z^*]\},\tag{4.7}$$

$$\partial\Omega=\{\underline{x}=(\xi(x_3)\cos(\phi),\xi(x_3)\sin(\phi),x_3)^T, (\phi,x_3)\in[0,2\pi)\times[-z^*,z^*]\},\tag{4.8}$$

where z^* is a positive constant and

$$\xi(x_3)=\frac{1}{2}(z^*-|x_3|),\quad -z^*\le x_3\le z^*.\tag{4.9}$$

Remind that (r_1,ϕ) are canonical polar coordinates in the (x_1,x_2) plane. Note that the double cone given in (4.7) has center of mass in the origin and has the x_3-axis as cylindrical symmetry axis. In the following experiment we choose $z^*=2$ and we denote with $\underline{x}_\xi(\phi,x_3)$ a point of the surface $\partial\Omega$.

Let z_r, z_c, v_r, v_c be positive constants such that $z_c<z_r\le z^*$, $v_c\le v_r$, $v_c<z_c$, $v_r<z_r$ the surfaces $\partial\Omega_c$ and $\partial\Omega_r$ are chosen as done in (4.8) where we replace ξ respectively with ξ_c and ξ_r given by the following formulae:

$$\xi_c(x_3)=\begin{cases}\dfrac{1}{2}(z_c-|x_3|) & v_c<|x_3|\le z_c,\\ \dfrac{1}{2}\left(z_c-\dfrac{v_c}{2}-\dfrac{x_3^2}{2v_c}\right) & |x_3|\le v_c,\end{cases}\tag{4.10}$$

$$\xi_r(x_3)=\begin{cases}\dfrac{1}{2}(z_r-|x_3|) & v_r<|x_3|\le z_r,\\ \dfrac{1}{2}\left(z_r-\dfrac{v_r}{2}-\dfrac{x_3^2}{2v_r}\right) & |x_3|\le v_r.\end{cases}\tag{4.11}$$

We note that in this experiment we have chosen $u^i_{\omega^*}(\underline{x}_\xi(\phi,x_3))=\exp(-\imath k^* x_3)$, $(\phi,x_3)\in[0,2\pi)\times[-z^*,z^*]$ so that we have explicit formulae for the coefficients of the field $u^i_{\omega^*}(\underline{x}_\xi)$ in the basis $\widehat{W}^2_{2,1/2}((0,2\pi)\times(-z^*,z^*))$. Thank to these explicit formulae we can study how we should increase the multi-resolution scale m^*, when the wave number k^* increases, that is when the ratio $R_T=2z^*/(2\pi)/k^*$ increases, to get a solution of the scattering problem of quality approximately independent of k^*. Let us denote with $g_{j,m,\nu,j',m',\nu'}$, $j=-2,-1$, $m=0$, $\nu=0$, $j=0,1$, $m=0,1,\cdots,m^*$, $\nu=0,1,\cdots,2^m-1$, $j'=-2,-1$, $m'=0$, $\nu'=0$, $j'=0,1$, $m'=0,1,\cdots,m^*$, $\nu'=0,1,\cdots,2^{m'}-1$ the coefficients in the basis $\widehat{W}^2_{2,1/2}((0,2\pi)\times(-z^*,z^*))$ of $u^i_{\omega^*}(\underline{x}_\xi)$, we have:

$$\begin{aligned}g_{j,m,\nu,j',m',\nu'}=&\frac{1}{\sqrt{2\pi}}\int_0^{2\pi}d\phi\,\widehat{\psi}^2_{j,m,\nu,2,1/2}\left(\frac{\phi}{2\pi}\right)\\&\times\frac{1}{\sqrt{2z^*}}\int_{-z^*}^{z^*}dx_3\exp(-\imath k^* x_3)\,\widehat{\psi}^2_{j',m',\nu',2,1/2}\left(\frac{(x_3+z^*)}{2z^*}\right),\end{aligned}\tag{4.12}$$

and let us denote with $g^Q_{j,m,\nu,j',m',\nu'}$ the approximation of the coefficient $g_{j,m,\nu,j',m',\nu'}$ obtained computing numerically the integral (4.12) using in each variable the composite Q points Gauss-Legendre quadrature rule (two subintervals in the support of the wavelet functions are considered). Let $I_{2,2,m^*}$ be the set defined in (3.23) and let $u^i_{m^*}(\phi,x_3)$, and $u^i_{Q,m^*}(\phi,x_3)$ be the approximations of $u^i(\underline{x}_{\tilde{\xi}}(\phi,x_3))$ obtained summing the wavelet expansion using the coefficients (4.12) and the coefficients $g^Q_{j,m,\nu,j',m',\nu'}$. Furthermore, let

$$x_{i,j}=(\xi(x_{3,i})\cos(\phi_j),\xi(x_{3,i})\cos(\phi_j),x_{3,i})^T\in\mathbb{R}^3,\quad i,j=1,2,\cdots,15,$$

be a grid of points belonging to $\partial\Omega$, with $x_{3,i}=-z^*+0.001+(2i-1)z^*/15$, and $\phi_j=(2j-1)\pi/15$. We define the following two quantities:

$$e_{k,m^*}=\frac{1}{\lambda}\sqrt{\sum_{i=1}^{15}\sum_{j=1}^{15}\left|u^i(\underline{x}_{\tilde{\xi}}(\phi_j,x_{3,i}))-u^i_{m^*}(\phi_j,x_{3,i})\right|^2},\tag{4.13}$$

$$w^Q_{k,m^*}=\frac{1}{\lambda}\sqrt{\sum_{i=1}^{15}\sum_{j=1}^{15}\left|u^i(\underline{x}_{\tilde{\xi}}(\phi_j,x_{3,i}))-u^i_{Q,m^*}(\phi_j,x_{3,i})\right|^2},\tag{4.14}$$

where $\lambda=\sqrt{\sum_{i=1}^{15}\sum_{j=1}^{15}|u^i(\underline{x}_{\tilde{\xi}}(\phi_j,x_{3,i}))|^2}$.

We note that e_{k,m^*} measures how accurate is the wavelet expansion in the approximation of the incoming wave and w^Q_{k,m^*} measures the accuracy of the wavelet expansion as a function of the quadrature rule used to compute the coefficients (4.12). The difference $|e_{k,m^*}-w^Q_{k,m^*}|$ measures the error due to the use of the quadrature rule.

Table 3 shows from left to right the wave number k^*, the ratio R_T, the number of unknowns used $J_{2,2,m^*}$ and the quantities e_{k,m^*}, w^4_{k,m^*}, w^8_{k,m^*}, w^{12}_{k,m^*}. Note that the choices of $J_{2,2,m^*}$ proposed in Table 3 guarantee that we have always $e_{k,m^*}\leq 5\cdot 10^{-2}$.

Table 3 makes possible to choose as a function of the ratio R_T the quadrature formula and the number of unknowns that must be used to compute a solution of the scattering problem of quality approximately independent of R_T. We consider adequate a quadrature rule for the discretization of the boundary integral equation when e_{k,m^*} is of the same order of magnitude of w^Q_{k,m^*}.

We note that when R_T increases we must increase the number of the quadrature nodes to get satisfactory approximations. In the experiments with large values of R_T, in order to avoid the use of quadrature rules with a large number of nodes, we could use asymptotic expansions as R_T goes to infinity of the integrals involved. The expansions when R_T goes to infinity correspond to the expansions when k^* goes to infinity since the obstacle considered is fixed.

To understand the behavior of the condition number of the matrix $A^{k,M}$, $M=2$, of the linear system (3.27) when k increases we compute the Green's function $\tilde{\Phi}(r)=e^{\imath kr}/(4\pi r)$ as a function of r, $0<r<r_{max}$, where r_{max} is a sufficiently large positive constant (see (1.6))

Table 3: Example 4.2: Analysis of the wavelet series expansion of the incoming field.

k^*	R_T	$J_{2,2,m^*}$	e_{k,m^*}	w^4_{k,m^*}	w^8_{k,m^*}	w^{12}_{k,m^*}
$\pi/2$	0.5	256	2.31e-02	2.31e-02	2.31e-02	2.32e-02
$\pi/2$	0.5	1024	5.81e-03	5.82e-02	5.82e-02	5.82e-03
π	1	1024	2.31e-02	2.40e-02	2.31e-02	2.31e-02
π	1	4096	5.78e-03	8.45e-03	5.78e-03	5.78e-03
2π	2	4096	2.29e-02	2.28e-01	2.29e-02	2.29e-02
2π	2	16384	5.72e-03	2.36e-02	5.72e-03	5.72e-03
4π	4	16384	2.27e-02	8.18e-01	7.401e-02	2.27e-02
4π	4	65536	5.67e-03	8.15e-01	7.38e-02	5.67e-03
8π	8	65536	2.25e-02	1.13e+00	4.47e-01	5.38e-01
8π	8	262144	5.83e-03	1.13e+00	4.50e-01	5.36e-01
32π	32	262144	9.02e-02	1.23e+00	4.05e-01	3.14e-01
32π	32	1048576	2.31e-02	1.21e+00	4.01e-01	3.01e-01

via its expansion in the Haar's wavelet basis. Note that the coefficients of this expansion can be computed explicitly.

Table 4 shows the L_1-condition numbers c_G, c_H computed with the IMSL DLFCCG routine of the matrix $A^{k,2}$ obtained computing the matrix elements evaluating the appropriate integrals using the Green's functions $\Phi(\underline{x}_{\xi_r},\underline{x}_{\xi_c})$ (see (4.10), (4.11) and recall that $\Phi(\underline{x}_{\xi_r},\underline{x}_{\xi_c})=\tilde{\Phi}(\|\underline{x}_{\xi_r}-\underline{x}_{\xi_c}\|)$) or evaluating the same integrals using the expansion of the Green's function in the Haar basis respectively for two values of k, $k=4\pi$, 16π and three value of $J_{2,2,m^*}$, $J_{2,2,m^*}=256,1024,4096$. Note that in this experiment we choose $z_r=2-\epsilon_r$, $\epsilon_r=0.01$, $z_c=2-\epsilon_c$, $\epsilon_c=0.2$, $v_r=v_c=0.25$. Indeed to keep the condition number small when $J_{2,2,m^*}$ increases we should decrease the parameters ϵ_c and v_r, v_c. Table 4 shows that the condition numbers c_H, that is the condition numbers relative to the matrix obtained integrating the Haar expansion of the Green's function, are smaller than the corresponding condition numbers c_H of the matrix obtained integrating directly the Green's function.

Note that when $J_{2,2,m^*}$ increases the corresponding condition number increases rapidly since we take the value of v_r, v_c, ϵ_r, ϵ_c fixed. As said above in order to keep small the condition number we should decrease these parameters. We do not do this to put in evidence the fact that the evaluation of the matrix elements obtained integrating the Haar expansion of the Green's function generates matrices less sensible to the choices of the remaining parameters.

After this first analysis we continue the study of the double cone example studying how the method proposed approximates the solution of the time harmonic scattering problem. We consider $k^*=\omega^*/c=2\pi$, $c=1$ and we approximate the density v_k appearing in (1.5) relative to the solution of the scattering problem considered with the function obtained truncating the series expansion (3.14) at $s=S$ ($S=0$ or $S=1$) and solving the linear systems (3.27), that is the linear systems (3.33) with the threshold $\tau=0$. Remember

Table 4: Example 4.2: Condition numbers.

$k=4\pi, R_T=8$			$k=16\pi, R_T=32$		
$J_{2,2,m^*}$	c_G	c_H	$J_{2,2,m^*}$	c_G	c_H
256	1.955e+04	1.597e+04	256	1.571e+05	2.158e+04
1024	3.211e+09	2.715e+05	1024	4.670e+10	4.013e+05
4096	1.21e+21	1.991e+06	4096	1.236e+21	6.639e+06

that with these choices $R_T=4$.

In this experiment and in the following ones we use as unknown the density v_k multiplied by the function $\sqrt{g_c(\underline{v})}$, $\underline{v}\in\tilde{I}_2\times\tilde{I}_3$ (see (3.12)). That is in (3.18) the function $\sqrt{g_c(\underline{v})}$ has been removed from the kernel (3.17) and has been considered included in the unknown so that the linear systems (3.27) and (3.33) should be reinterpreted coherently with this choice. This trick improves the accuracy of the approximate solution since it acts as a kind of regularization of the integral equation.

We remind that the numerical approximation $u^s_{k,S,m^*,\tau}$ of u^s_k obtained with the numerical method of Section 3 satisfies by construction the Helmholtz equation (1.1) and the boundary condition at infinity (1.4). So that we must study only how $u^s_{k,S,m^*,\tau}$ satisfies the boundary condition (1.2). Remind that in this experiment since $\partial\Omega_2=\emptyset$ the boundary condition (1.3) should not be considered. We define the following quantities:

$$V_1=\left(\int_{\partial\Omega_1} ds(\underline{x})\left|g_{1,k}(\underline{x})-u^s_{k,S,m^*,\tau}(\underline{x})\right|^2\right)^{1/2}, \tag{4.15}$$

$$V_2=\left(\int_{\partial\Omega_1} ds|g_{1,k}|^2\right)^{1/2}, \quad e_{k,S,m^*,\tau}=\frac{V_1}{V_2}. \tag{4.16}$$

Note that in the problem considered we have: $g_{1,k}(\phi,x_3)=-\exp(-\imath k^* x_3)$. The quantity $e_{k,S,m^*,\tau}$ defined in (4.16) is a measure of how well the numerical approximation $u^s_{k,S,m^*,\tau}$ of u^s_k satisfies the boundary condition (1.2) on $\partial\Omega$. In Table 5 from left to right we show the value of m^*, the number of unknowns used $J_{2,2,m^*}=2^{2(m^*+2)}$, the quantities e_{k,m^*}, $e_{k,S,m^*,0}$ and the constants z_c, z_r, v_c, v_r. Table 5 shows the behavior of $e_{k,S,m^*,0}$ as a function of the number of unknowns used and of the order of the expansion S.

Table 5 shows that the correction due to the first order term of the perturbation expansion makes the error $e_{k,S,m^*,0}$ on the boundary condition of the same order of magnitude of the error e_{k,m^*}, that is the error due to the representation formula of the datum via the truncated wavelet expansion and this is very satisfactory since this is the best result that can be obtained.

Example 4.3. The third experiment involves a simplified version of the "submarine" (see Fig. 1(b)). The data of this obstacle are derived from the data shown in Fig. 1(a). The data of Fig. 1(a) represent a United States Navy submarine of the Los Angeles class and are available at the website: *http://avalon.viewpoint.com/*.

Table 5: Example 4.2: Accuracy in satisfying the boundary condition on the double cone: perturbative approach.

m^*	$2^{2(m^*+2)}$	e_{k,m^*}	$e_{k,S,m^*,0}$	z_c	z_r	v_c	v_r
S=0							
0	16	9.662e-01	9.993e-01	1.5	2	0.5	0.5
1	64	8.406e-01	9.987e-01	1.7	2	0.5	0.5
2	256	3.241e-01	7.544e-01	1.9	2	0.5	0.5
3	1024	9.000e-02	7.102e-01	1.95	2	0.2	0.2
4	4096	2.593e-02	7.085e-01	1.975	2	0.1	0.1
$S=1$							
0	16	9.662e-01	9.660e-01	1.5	2	0.5	0.5
1	64	8.406e-01	8.401e-01	1.7	2	0.5	0.5
2	256	3.241e-01	3.641e-01	1.9	2	0.5	0.5
3	1024	9.000e-02	1.201e-01	1.95	2	0.2	0.2
4	4096	2.593e-02	4.098e-02	1.975	2	0.1	0.1

The most natural coordinate system to represent this obstacle (see Fig. 1(a)) and to build the associate operator expansion seems to be a cylindrical coordinate system with cylindrical axis given by the symmetry axis of the main body of the submarine. However, an analysis of the boundary of the submarine (see Fig. 1(a)) shows that the boundary of the submarine is not representable with a single valued function in these cylindrical coordinates. So that we have modified the original data shown in Fig. 1(a) to obtain the data shown in Fig. 1(b), this last data set represents the so called simplified version of the "submarine". In the numerical experiments we have used as obstacle a scaled model of the "submarine" of Fig. 1(b), that is the physical dimensions of the submarine are divided by a factor 11.03 so that the maximum length of the real submarine that is 110.3*meters* in the scaled model corresponds to 10 *units* (1 *unit*=11.03 *meters*). Coherently we have chosen $c=(1532.8/11.03)\,units/seconds$, which corresponds to re-scaling the sound speed in the sea water (i.e., sound speed in the sea water equal to 1532.8 *meters*/*seconds*) and we have chosen the $v_3=x_3$ axis of the cylindrical coordinate system as the symmetry axis of the main body of the submarine oriented with the positive direction going out of the prow of the submarine. Due to the scale (1:11.03) and to the choice of the origin on the x_3 axis, we have that the minimum and the maximum values reached by the boundary of the simplified submarine on the $v_3=x_3$ axis are $x_{3,min}=-5units$, $x_{3,max}=5units$ respectively. The remaining axes are chosen taking a dextrorse coordinate system in the plane orthogonal to the $v_3=x_3$ axis. Moreover we have chosen $\partial\Omega_1=\partial\Omega$, $\partial\Omega_2=\emptyset$, and

$$\chi(\underline{x})=\begin{cases} 0, & \underline{x}\in\partial\Omega \quad \text{and} \quad |x_3-1.2|<1 \text{ or } |x_3^2-25|<0.5, \\ 2, & \text{otherwise.} \end{cases} \tag{4.17}$$

This choice of χ makes the obstacle "soft" in the "prow", the "turret" and the "beams", that is we try to model the fact that the submarine is coated in the locations mainly re-

sponsible for the scattering phenomenon. Let ξ be a function such that the boundary of the simplified version of the submarine, that is the $\partial\Omega$ of this experiment, is given by

$$v_1=\xi(\underline{v}),\quad \underline{v}=(v_2,v_3)^T,\quad v_2=\phi,\quad v_3=x_3,$$

and

$$\underline{x}=(\xi(\underline{v})\cos(v_2),\xi(\underline{v})\sin(v_2),v_3)^T,\quad \underline{v}\in[0,2\pi)\times[-5,5].$$

Furthermore we choose $\tilde{I}_2\times\tilde{I}_3=(0,2\pi]\times[-5+\epsilon_1,5-\epsilon_1]$, $\hat{I}_2\times\hat{I}_3=(0,2\pi]\times[-5,5]$ with $0<\epsilon_1\ll 1$ and we choose ξ_c, ξ_r in such a way that $\partial\Omega_c$, $\partial\Omega_r$ are "slimmer" versions in the $v_1=r_1$ coordinate of $\partial\Omega$. In other words, $\xi_c(\underline{v})$, $\underline{v}\in\hat{I}_2\times\hat{I}_3$ and $\xi_r(\underline{v})$, $\underline{v}\in\tilde{I}_2\times\tilde{I}_3$ are suitable piecewise linear interpolations of $\xi(\underline{v})-\epsilon_1$, $\underline{v}\in\hat{I}_2\times\hat{I}_3$ and $\xi(\underline{v})-\epsilon_2$, $\underline{v}\in\tilde{I}_2\times\tilde{I}_3$, with $0<\epsilon_2<\epsilon_1\ll 1$ respectively.

We consider the time dependent scattering problem (1.9)-(1.15), where the incident wave u^i is given by:

$$u^i(\underline{x},t)=e^{-\frac{1}{4\zeta^2}[(\underline{\gamma},\underline{x})-ct]^2}=\frac{\zeta}{\sqrt{\pi}}\int_{\mathbb{R}}e^{-\zeta^2\omega^2}e^{\left(\frac{\imath\omega}{c}[(\underline{\gamma},\underline{x})-ct]\right)}d\omega,\quad(\underline{x},t)\in\mathbb{R}^3\times\mathbb{R},\quad(4.18)$$

with $\zeta=0.25$, $\underline{\gamma}=(0,0,-1)^T$ and $c=(1532.8/11.03)\,units/seconds$.

Since u^i is given by formula (4.18) similarly the scattered field u^s can be represented by the following one-dimensional integral:

$$u^s(\underline{x},t)=\frac{\zeta}{\sqrt{\pi}}\int_{\mathbb{R}}e^{-\zeta^2\omega^2}e^{-\imath\omega t}u^s_{\omega,\underline{\gamma}}(\underline{x})d\omega,\quad(\underline{x},t)\in(\mathbb{R}^3\setminus\overline{\Omega})\times\mathbb{R}.\quad(4.19)$$

Note that the integrals (3.37) and (3.38) reduce to the integrals (4.18) and (4.19) when we choose $w(\omega)=((2\pi)^4\zeta/\sqrt{\pi})e^{-\zeta^2\omega^2}$, $\omega\in\mathbb{R}$, $W(\omega,\underline{\alpha})=\delta(\underline{\alpha}-\underline{\gamma})$ where $\delta(\cdot)$ is the Dirac's delta on ∂B concentrated in $\underline{\alpha}=\underline{\gamma}$. We approximate the integrals (4.18) and (4.19) with the Gauss-Hermite quadrature rule. Note that even if the integral appearing in (4.18) can be done explicitly it will be approximated using the Gauss-Hermite quadrature rule in order to choose some parameters appearing in the rest of the computation. More precisely, in (1.16) we choose $N_2=1$, $\underline{\alpha}_1=\underline{\gamma}$ and for $i=1,\cdots,N_1$ we choose $p_{i,1}$, $\zeta\omega_i$, to be the weights and the nodes of the Gauss-Hermite quadrature formula respectively. In the experiment involving the incoming wave (4.18) we choose $N_1=400$ in (1.16). This choice is based on a criterion similar to the one used in ([6], p. 1835). The choice of ζ and of the quadrature rule made implies that the ratios R_T between the physical dimensions of the obstacles ($10\,units$) and the wavelengths of the time harmonic waves used to approximate the wave packet (4.19) (contained in the interval $0.725\,units$-$6.346\,units$) range between 1.5 and 13. We start using 256 (complex) unknowns to solve the corresponding time harmonic problem when $R_T=10/6.34\approx 1.57$ is at its minimum value and we use 4096 (complex) unknowns when R_T reaches its maximum value $R_T=10/0.725\approx 13.79$. Finally we choose $S=1$, $\tau=0$.

Fig. 3 shows in the first column the incident wave and in the second column the wave scattered by the simplified version of the submarine for three values of the time, that is:

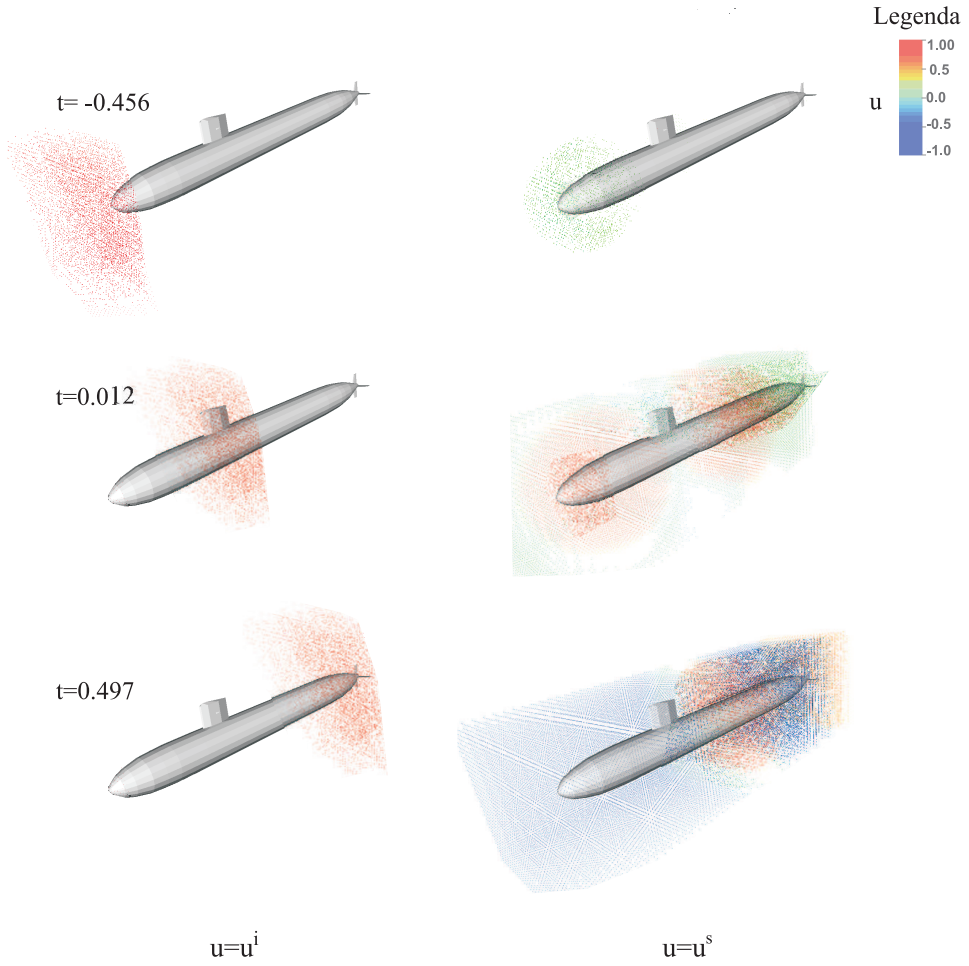

Figure 3: Time dependent scattering from the simplified version of the submarine.

$t_1 = -0.456$, $t_2 = 0.012$, $t_3 = 0.497$. Fig. 3 shows that when the incident wave goes through the obstacle the energy is irradiated essentially by the "turret" and by the "prow" and then by the "beams" of the "stern". Note that the energy irradiated by the "prow" when hit by the incident wave corresponds initially to negative values of u^s (blue colour) (see Fig. 3, $t = t_1$). In fact the "prow" is coated and behaves as an acoustically soft obstacle. The same happens with the "turret" (see Fig. 3, $t = t_2$). On the contrary the part of the simplified submarine placed between the "turret" and the "beams" has an impedance χ equal to 2, that is almost acoustically hard, so that the energy irradiated when it is hit by the incident wave corresponds initially to positive values of u^s (see Fig. 3, $t = t_2$ red colour). Note that the energy irradiated by the "beams" of the "stern" is comparable with the energy scattered by the "turret" or the "prow" of the submarine (see Fig. 3, $t = t_3$). This is due to the fact that the incident wave packet contains waves whose wavelengths are comparable with the characteristic dimensions of the "beams". In [1], Section IV is

shown the scattering on the (simplified) submarine of an incident wave packet containing harmonic waves whose wavelength is large compared with the characteristic dimension of the "beams". In this case the "beams" irradiate very little energy .

Example 4.4. The fourth experiment concerns the simplified version of the NASA space shuttle (see Fig. 2(b)). The data of the NASA space shuttle are available in the website *http://avalon.viewpoint. com/*.

As in the case of the submarine (see Fig. 1) the most natural coordinate system to represent this obstacle and to build the operator expansion seems to be a cylindrical coordinate system with cylindrical axis given by the symmetry axis of the main body of the shuttle. However, the surface of the NASA space shuttle (see Fig. 2(a)) is not representable with a single valued function in this coordinate system so that we have modified the original data shown in Fig. 2(a) in order to fulfill the assumptions (3.1) and (3.2) and we have obtained the data shown in Fig. 2(b), which is a simplified version of the NASA space shuttle.

The reference surface $\partial\Omega_r$ and the internal surface $\partial\Omega_c$ have been obtained manipulating the original 3D model shown in Fig. 2(a) with a CAD program named Rhinoceros [30] and exporting the data of the surfaces obtained as a file of type RAW, that is a file containing the cartesian coordinates of the vertices of the triangles of a surface triangulation. The points of the surfaces generated in this way have been interpolated using splines of second or fourth order according with the number of vanishing moments M chosen in the wavelet basis used.

In the numerical experiment we have considered a "scaled" model of the "shuttle", that is the physical dimensions of the shuttle are expressed in *units* where $1 unit = (56.14/14)$ *meters*. The maximum length of the shuttle corresponds to $14 units$. The sound speed in the air $331.45 meters/seconds$ expressed in $units/seconds$ is c=$82.65 units/seconds$. Finally, as done for the submarine we have chosen $\underline{v}_3 = x_3$, the axis of the cylindrical coordinate system, to be the symmetry axis of the main body of the simplified shuttle. The $v_3 = x_3$ axis is oriented with the positive direction going out of the prow of the NASA space shuttle. Due to the scale (1:(56.14/14)) and to the position of the origin on the x_3 axis the minimum and the maximum values reached by the boundary of the simplified shuttle on the x_3 axis are $x_{3,min} = -7 units$, $x_{3,max} = 7 units$ respectively.

We choose $\partial\Omega_1 = \emptyset$, $\partial\Omega_2 = \partial\Omega$ and $\chi(\underline{x}) = +\infty$, $\underline{x} \in \partial\Omega_2$. We omit the expression of the surfaces ξ_r and ξ_c since they are involved. These surfaces are "slimmer" versions of the boundary of the obstacle in Fig. 2(b) obtained reducing the size of the obstacle through a rescaling procedure but maintaining its proportions. In this experiment we consider a time harmonic wave $u^i(\underline{x},t) = e^{-\imath\omega^* t} e^{\imath(\omega^*/c)(\underline{\alpha}^*,\underline{x})}$, where $\alpha^* = (0,0,-1)^T$ and $\omega^*/c = 8\pi(unit)^{-1}$, that is the ratio R_T is equal to 56. We have chosen $m^* = 7$, that is the real dimension of the linear systems involved in the computation is $2^{19} \times 2^{19} (= 524288 \times 524288)$, and truncation parameter $\tau = 10^{-5}$.

Fig. 4 shows the results of the time harmonic scattering of the modified version of the space shuttle when hit by the incoming wave. As in Fig. 3 the first column shows the

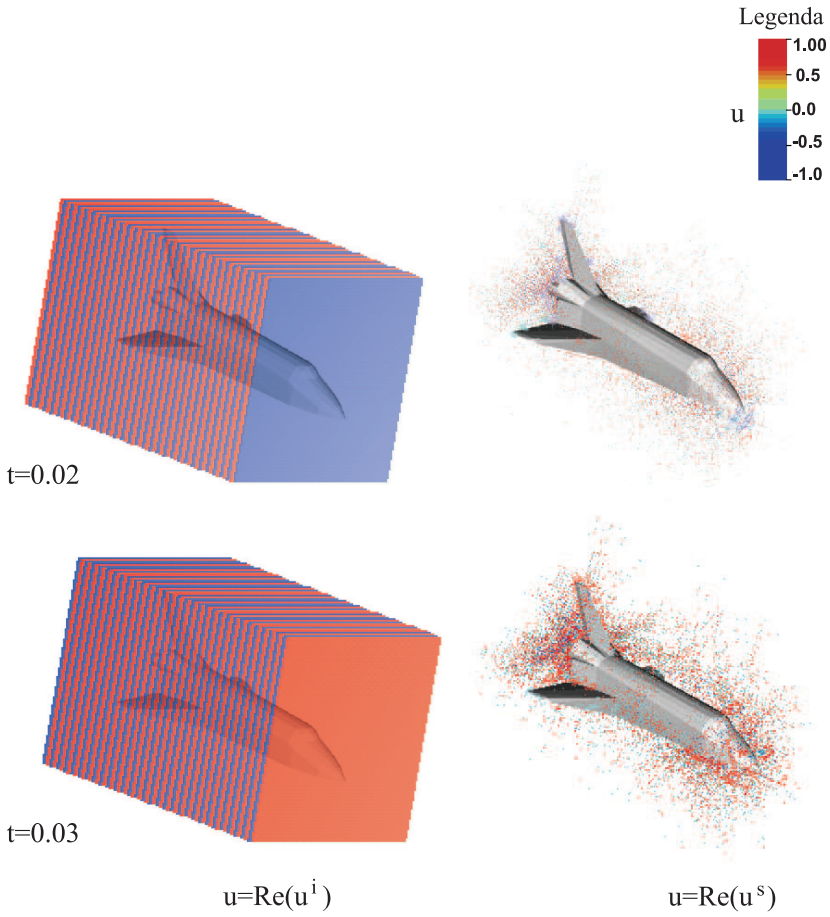

Figure 4: Time harmonic scattering from the simplified version of the NASA space shuttle.

real part of the incident wave and the second column shows the real part of the scattered wave. Note that since the simplified shuttle is an acoustically hard obstacle the field scattered by the obstacle is of the same sign of the incoming field. Due to the large value of R_T the real part of the incoming wave presents narrow packets where the wave changes from being positive to being negative compared to the dimension of the obstacle, so that in each portion of space of the size of one packet around the simplified version of the shuttle we can see a scattered field of positive and negative sign. In particular this phenomenon is more evident in the "prow" and in the "tails" (see Fig. 4). Furthermore for reason similar to those explained in the third experiment the choice of R_T made in this experiment is responsible for the fact that the "engine" and the "tail" scatter as much as the prow of the shuttle.

In the website *http://www.econ.univpm.it/recchioni/w12* we show some animations and virtual reality applications relative to the numerical experience presented. More

general references to the work of the authors in scattering can be found in *http://www.econ.univpm.it/recchioni/scattering*

Acknowledgments

The numerical experience reported in this paper has been obtained using the computing grid of Enea (Roma, Italy). The support and sponsorship of Enea (Roma, Italy) is gratefully acknowledged.

A Appendix

Lemma A.1. *Let $N=2$ and T_m, $m=0,1,\cdots$ be the following closed subspaces of $L^2((0,1))$:*

$$T_m=\{f\in L^2((0,1))\,|\,f(x)=p_\nu,\, x\in(\nu N^{-m},(\nu+1)N^{-m}),\\ p_\nu\in\mathbb{R},\nu=0,1,\cdots,N^m-1\},\quad m=0,1,\cdots. \tag{A.1}$$

Then we have:

$$T_0\subset T_1\subset T_2\subset T_3\subset\cdots, \tag{A.2}$$

$$\cap_{m=0}^{\infty}T_m=P^1((0,1)), \tag{A.3}$$

$$\overline{\cup_{m=0}^{\infty}T_m}=L^2((0,1)). \tag{A.4}$$

Proof. Properties (A.2), (A.3) can be easily derived from (A.1). The proof of (A.4) follows from the density of the piecewise constant functions in $L^2((0,1))$ (see [25] Theorem 3.13 p. 84). This concludes the proof. □

Note that for $m=0,1,\cdots$ the fact that $f(x)\in T_m$ implies that for $\nu=0,1,\cdots,N^m-1$ as a function of x for $x\in(0,1)$ $\tilde{f}_{\nu,m}(x)=f(N^m x-\nu)\in T_0$.

Theorem A.1. *Let $N=2$, $\psi^M_{j,m,\nu,N,\underline{\eta}^N}(x)$, $x\in(0,1)$, be the functions defined in* (2.8)*. Then we have*

$$\int_0^1 dx\,\psi^M_{j,m,\nu,N,\underline{\eta}^N}(x)x^p=0,\quad p=0,1,\cdots,M-1,\quad(\nu,m,j)\in\Lambda, \tag{A.5}$$

where Λ is defined in (2.8b)*, and*

$$\int_0^1 dx\,\psi^M_{j,m,\nu,N,\underline{\eta}^N}(x)\psi^M_{j',m',\nu',N,\underline{\eta}^N}(x)=\begin{cases}0, & m\neq m' \text{ or } \nu\neq\nu' \text{ or } j\neq j',\\ 1, & m=m' \text{ and } \nu=\nu' \text{ and } j=j',\end{cases} \tag{A.6a}$$

$$\nu=0,1,\cdots,N^m-1,\quad \nu'=0,1,\cdots,N^{m'}-1,\quad m,m'=0,1,\cdots,\quad j,j'=0,1,\cdots,M-1. \tag{A.6b}$$

Proof. Property (A.5) follows from definition (2.8) and equation (2.6). The proof of (A.6) follows from equation (2.7) when $m=m'$, $\nu=\nu'$ and $j\neq j'$ and from the fact that the supports of the functions $\psi^M_{j,m,\nu,N,\underline{\eta}^N}$ and $\psi^M_{j',m',\nu',N,\underline{\eta}^N}$ are either disjoint sets or sets contained

one into the other. In particular, when $m=m'$ and $\nu\neq\nu'$ the supports are disjoint and when $m\neq m'$, let us suppose for example $m>m'$, the supports are either disjoint sets or sets contained one into the other depending on the values of the indices ν and ν'. When the supports are disjoint condition (A.6) is obvious, when the supports are contained one into the other condition (A.6) follows from (A.5). Finally when $m=m'$, $\nu=\nu'$, $j=j'$ condition (A.6) follows from Eq. (2.7). This concludes the proof. □

Theorem A.2. *For $N=2$, the set $W^M_{N,\underline{\eta}^N}((0,1))$ defined in* (2.9) *is an orthonormal basis of $L^2((0,1))$.*

Proof. The set $W^M_{N,\underline{\eta}^N}((0,1))$ is an orthonormal set of functions such that for $m=0,1,\cdots$ the subspace T_m defined in (A.1) is contained in the subspace generated by $W^M_{N,\underline{\eta}^N}((0,1))$. Then from Lemma A.1 it follows that $W^M_{N,\underline{\eta}^N}((0,1))$ is a basis of $L^2((0,1))$. This concludes the proof. □

Let us denote with $C^j((0,1))$, $j=0,1,\cdots$ the space of the real continuous functions defined on $(0,1)$ with the first j-derivatives continuous. Let $[0,1]$ be the closure of $(0,1)$ and let M_1 be a non-negative integer we denote with $C^{M_1}([0,1]\times[0,1])$ the space of the real continuous functions defined on $[0,1]\times[0,1]$ M_1-times continuously differentiable on $[0,1]\times[0,1]$. We have:

Lemma A.2. *Let $M\geq 1$ be an integer, $N=2$ and $W^M_{N,\underline{\eta}^N}((0,1))$ be the set given in* (2.9)*, and let $K(x,y)$, $(x,y)\in[0,1]\times[0,1]$ be a real function such that:*

$$K\in C^{M_1}([0,1]\times[0,1]),\quad M_1\geq M. \tag{A.7}$$

Moreover, let $\alpha_{m,\nu,j,m',\nu',j'}$ be the following quantities:

$$\alpha_{m,\nu,j,m',\nu',j'}=\int_0^1 dx\psi^M_{j,m,\nu,N,\underline{\eta}^N}(x)\int_0^1 dy\psi^M_{j',m',\nu',N,\underline{\eta}^N}(y)K(x,y), \tag{A.8}$$

where (m,m',ν,ν',j,j') satisfy (A.6b)*. Then there exists a positive constant D_M such that:*

$$|\alpha_{m,\nu,j,m',\nu',j'}|\leq\frac{D_M}{\left(N^{max(m,m')}\right)^{M+1}}, \tag{A.9}$$

where (m,m',ν,ν',j,j') satisfy (A.6b)*.*

Proof. The proof is analogous to the proof of Proposition 4.1 in [26], in fact condition (A.7) implies that there exists a positive constant C_M such that:

$$\left|\frac{\partial^M}{\partial x^M}K(x,y)\right|+\left|\frac{\partial^M}{\partial y^M}K(x,y)\right|\leq C_M,\quad (x,y)\in[0,1]\times[0,1]. \tag{A.10}$$

That is let N,j,j',ν,ν',m,m' be as above and (x^*,y^*) be the center of mass of the set $(\nu N^{-m},(\nu+1)N^{-m})\times(\nu' N^{-m'},(\nu'+1)N^{-m'})$. We use the Taylor polynomial of $f(y)=K(x,y)$, $y\in[0,1]$ of degree $M-1$ and base point $y=y^*$ when $m<m'$ or the Taylor polynomial of $g(x)=K(x,y)$, $x\in[0,1]$ with base point $x=x^*$, Eq. (A.5), assumption (A.10) and take into account the fact that the functions $\psi^M_{j,m,\nu,N,\underline{\eta}^N}$ and $\psi^M_{j',m',\nu',N,\underline{\eta}^N}$ have support in the sets $(\nu N^{-m},(\nu+1)N^{-m})$ and $(\nu' N^{-m'},(\nu'+1)N^{-m'})$, respectively. Using the remainder formula of the Taylor polynomial it is easy to see that the estimate (A.9) for $\alpha_{m,\nu,j,m',\nu',j'}$ holds. Note that the constant D_M depends on M, N, $\underline{\eta}^N$, C_M. This concludes the proof. □

Note that, as seen in Section 3, the estimate (A.9) is the basic property that together with a simple truncation procedure makes the wavelet bases introduced useful to approximate with sparse matrices the integral operators coming from the operator expansion method.

References

[1] M. C. Recchioni and F. Zirilli, The use of wavelets in the operator expansion method for time dependent acoustic obstacle scattering, SIAM J. Sci. Comput., 25 (2003), 1158-1186.

[2] J. Nečas, Les Méthodes Directes en Théorie des Équations Elliptiques, Masson & Cie. Publ., Paris, 1967.

[3] A. A. Ergin, B. Shanker and E. Michielssen, Fast evaluation of three-dimensional transient wave field using diagonal translation operators, J. Comput. Phys., 146 (1998), 157-180.

[4] R. Coifman, V. Rokhlin and S. Wandzura, The fast multipole method for wave equation: a pedestrian prescription, IEEE Antennas Propag. Mag., 35 (1993), 7-12.

[5] K. Aygun, B. Shanker, A. A. Ergin and E. Michielssen, A two-level plane wave time domain algorithm for fast analysis of EMC/EMI problems, IEEE T. EMC, 44 (2002), 152-164.

[6] E. Mecocci, L. Misici, M. C. Recchioni and F. Zirilli, A new formalism for time dependent wave scattering from a bounded obstacle, J. Acoust. Soc. Am., 107 (2000), 1825-1840.

[7] R. Kress and A. Mohsen, On the simulation source technique for exterior problems in acoustics, Math. Method. Appl. Sci., 8 (1986), 585-597.

[8] L. Fatone, M. C. Recchioni and F. Zirilli, Mathematical models and numerical methods to solve some problems in time dependent acoustic obstacle scattering, in: S.G. Pandalai (Ed.), Recent Research Developments in Acoustics, Transworld Research Network, Kerala, India, Vol. 1, 2003, pp. 229-254.

[9] I. Daubechies, Ten Lectures on Wavelets, SIAM, Philadelphia, Pennsylvania, 1992.

[10] D. Colton and R. Kress, Integral Equation Methods in Scattering Theory, J. Wiley & Sons Inc., New York, 1983.

[11] D. M. Milder, An improved formalism for wave scattering from rough surface, J. Acoust. Soc. Am., 89 (1991), 529-541.

[12] D. M. Milder, An improved formalism for electromagnetic scattering from a perfectly conducting rough surface, Radio Sci., 31 (1996), 1369-1376.

[13] L. Misici, G. Pacelli and F. Zirilli, A new formalism for wave scattering from a bounded obstacle, J. Acoust. Soc. Am., 103 (1998), 106-113.

[14] M. C. Recchioni and F. Zirilli, High performance algorithms for time dependent wave scattering from a bounded obstacle, in: Proc. 5th Euro SGI/CRAY MPP–Massive Parallel Processing Workshop, Bologna, Italy, 1999, (http://www.cineca.it/mpp-workshop/proceedings.htm).
[15] S. Piccolo, M. C. Recchioni and F. Zirilli, The time harmonic electromagnetic field in a disturbed half space: an existence theorem and a computational method, J. Math. Phys., 37 (1996), 2762-2786.
[16] L. Fatone, C. Pignotti, M. C. Recchioni and F. Zirilli, Time harmonic electromagnetic scattering from a bounded obstacle: an existence theorem and a computational method, J. Math. Phys., 40 (1999), 4859-4887.
[17] M. C. Recchioni and F. Zirilli, A new formalism for time dependent electromagnetic scattering from a bounded obstacle, J. Eng. Math., 47 (2003), 17-43.
[18] F. Mariani, M. C. Recchioni and F. Zirilli, The use of the Pontryagin maximum principle in a furtivity problem in time-dependent acoustic obstacle scattering, Wave. Random Media, 11 (2001), 549-575.
[19] L. Fatone, M. C. Recchioni and F. Zirilli, Some control problems for the Maxwell equations related to furtivity and masking problems in electromagnetic obstacle scattering, in: G. C. Cohen, E. Heikkola, P. Joly and P. Neittaanmaki (Eds.), Mathematical and Numerical Aspects of Wave Propagation. Waves 2003, Springer Verlag, Berlin, 2003, pp. 189-194.
[20] L. Fatone, M. C. Recchioni and F. Zirilli, A masking problem in time dependent acoustic obstacle scattering, Acoust. Res. Lett. Online, 5(2) (2004), 25-30.
[21] L. Fatone, M. C. Recchioni and F. Zirilli, Furtivity and masking problems in time dependent electromagnetic obstacle scattering, J. Optimiz. Theory Appl., 121 (2004), 223-257.
[22] L. Fatone, M. C. Recchioni and F. Zirilli, Mathematical models of "active" obstacles in acoustic scattering, in: J. Cagnol and J. P. Zolesio (Eds.), Control and Boundary Analysis, Lecture Notes in Pure and Applied Mathematics 240, Marcel Dekker/CRC Press, Boca Raton, 2005, pp. 119-129.
[23] S. Mallat, Multiresolution approximation and wavelets, T. Am. Math. Soc., 315 (1989), 69-88.
[24] Y. Meyer, Ondelettes, fonctions splines et analyses graduées, Rend. Sem. Mat. Univ. Politec. Torino, 45 (1988), 1-42.
[25] W. Rudin, Real and Complex Analysis, McGraw Hill Inc., New York, 1966.
[26] G. Beylkin, R. R. Coifman and V. Rokhlin, Fast wavelet transforms and numerical algorithms I, Commun. Pur. Appl. Math., 44 (1991), 141-183.
[27] E. Giladi and J. B. Keller, A hybrid numerical asymptotic method for scattering problems, J. Comput. Phys., 174 (2001), 226-247.
[28] O. P. Bruno, Fast, high order, high frequency integral methods for computational acoustics and electromagnetics, in: Lectures Notes in Computational Science and Engineering, Springer-Verlag, Berlin, Vol. 31, 2003, pp. 43-82.
[29] D. Colton and R. Kress, Inverse Acoustic and Electromagnetic Scattering Theory, Springer Verlag, Berlin, 1992.
[30] Rhinoceros, NURBS Modeling for Windows, 3rd ed., Robert McNeel & Associates, USA, 2003, (http://www.rhino3d.com/).